

**GPR and bulk ground resistivity surveys in graveyards: locating
unmarked burials in contrasting soil types**

James D. Hansena, Jamie K. Pringlea* & Jon Goodwinb

aSchool of Physical Sciences & Geography, Keele University, Keele,
Staffordshire, ST5 5BG, UK.

bStoke-on-Trent Archaeology Service, Civic Centre, Stoke-on-Trent ST4 1HH,
U.K.

E-mail addresses; j.d.hansen@keele.ac.uk (J. Hansen),
j.k.pringle@keele.ac.uk (J. Pringle) & jon.goodwin@stoke.gov.uk (J. Goodwin)

*corresponding author. Tel: +44 (0)1782 733163. Fax: +44 (0)1782 733737,
Email: j.k.pringle@keele.ac.uk

Abstract

With graveyards and cemeteries globally being increasingly designated as full, there is a growing need to identify unmarked burial positions to find burial space or exhume and re-inter if necessary. In some countries, for example the U.S. and U.K., burial sites are not usually re-used; however, most graveyard and cemetery records do not have maps of positions. One non-invasive detection method is near-surface geophysics, but there has been a lack of research to-date on optimal methods and/or equipment configuration. This paper presents three case studies in contrasting burial environments, soil types, burial styles and ages in the U.K. Geophysical survey results reveal unmarked burials could be effectively identified from these case studies that were not uniform or predicted using 225 MHz frequency antennae GPR 2D 0.5 m spaced profiles. Bulk ground electrical surveys, rarely used for unmarked burials, revealed 1 m probe spacings were optimal compare to 0.5 m, with datasets needing 3D detrending to reveal burial positions. Results were variable depending upon soil type; in very coarse soils GPR was optimal; whereas resistivity was optimal in clay-rich soils and both were optimal in sandy and black earth soils. Archaeological excavations revealed unmarked burials, extra/missing individuals from parish records and a variety of burial styles from isolated, brick-lined, to vertically stacked individuals. Study results evidence unmarked burial targets were significantly different from clandestine burials of murder victims which are used as analogues.

42

43

44 Keywords: graves; burials; geophysics; GPR; resistivity

45

1. Introduction

Globally graveyards and cemeteries are suffering from a chronic lack of burial space, for example in the UK there is a need to accommodate ~140,000 burials every year [1 Environment Agency, 2004], but a 2006 U.K. Government report listed less than ¼ of current burial grounds have room to accept new burials [2 U.K. Ministry of Justice 2006]. In addition, only 20% had designated land as yet unused, with them expected to be filled within 25-30 years [3 U.K. Ministry of Justice 2006]. In the same report comparatively shallow graves are even being utilised. There has been the rapid expansion of so-called 'green' burial sites, for example, for example over 200 created in the UK since 2004 [4 Jim *et al.* 2008]; these taking up some of the demand although having a variety of burial styles [5 Rumble 2010]. Re-use of existing graveyards and cemeteries is one solution, for example, burial regulation relaxations have been in force in London since 2005 [2 Ministry of Justice, 2006]. However, burial records, if present, rarely indicate burial positions, and even gravestones are not always reliable indicators as [6 Fiedler (2009)] documents; anecdotal information suggests some gravestones may have been rotated for optimal viewing from passing paths, or even moved. Different countries also have different rules on the removal of human remains, for example, the United States generally leave remains *in situ* in perpetuity, the United Kingdom have a 100 year burial rule whereas in Germany remains can be moved when only 25 years old. In order to determine the positions of unmarked burials, probing methods (see [7 Owsley, 1995]) would not be deemed considerate of religious and social

sensitivities, and thus the use of non-invasive detection techniques should be considered.

Other authors have used remote sensing methods including aerial photography and satellite imagery, to identify unmarked burials (e.g. see [8-9 Brilis et al. 2000a,b]), and thermal imaging equipment either mounted on aircraft [10 Dickinson, 1976] or hand-held (e.g. see [11 Statheropoulis et al. 2011]). [12 Ruffell et al. (2009) identified historic (150-160 years old) unmarked graves using aerial photographs and confirmed positions by subsequent geophysical surveying. Forensic geomorphology methods have also been utilised for burial detection [13 Ruffell & McKinley 2014]) Localised vegetation growth may also have different characteristics to background areas, for example, different species and with more or stunted growth [14-15 Killam, 2004; Dupras et al. 2006] that [16 Larson et al. (2011)] attributes to localised pH soil changes and differing ground characteristics. [17 Pringle et al. 2012a] give a comprehensive overview of current commonly-used terrestrial search methods and relevant case study examples.

One potential ground-based, non-invasive detection method is near-surface geophysics. Magnetic surveys are commonly used to detect near-surface geotechnical targets (see [18] Reynolds, 2011). Magnetic surveys for clandestine burials of murder victims have had varied grave detection success (see [19 Juerges et al. 2010], although detection using magnetics for ancient archaeological graves have been successful (e.g. see [20 Linford 2004])). [21 Ellwood 1990] and [22 Witten et al. 2001] encountered difficulties in locating

19th century graves in cemeteries and a mass grave from 1921, respectively, using magnetic methods. Above-ground sources of magnetic interference seem to cause significant issues with this technique as [17] Pringle et al. (2012a) note. [23 Stanger and Roe 2007] showed fluxgate gradiometry equipment were successful to detect 20th century graves in an Australian cemetery.

Electro-magnetic (EM) surveys have shown to have variable detection success; [24 Frohlich and Lancaster (1986)] did locate and characterise unmarked burials in Jordan, with resulting target(s) contrasts with background levels dependent on the proportion of silt present within the graves. [25 Nobes (1999)] attempted to locate unmarked graves in a New Zealand cemetery, but was largely unsuccessful due to differentiating anomalies from background effects caused by both fence boundaries and local topography. [26 Bigman (2012)] undertook an EM survey over historic North American Indian burial grounds and identified over 60 anomalies, where previous excavations had found burials >2m bgl; but here there were no above-ground interfering structures present. Interestingly [25] Nobes (1999) found that the 'head' ends of unmarked graves were easier to identify than the 'foot' ends for reasons that were unclear. [27] Nobes (2000) was also successful in locating a 12 year old unmarked clandestine burial of a murder victim in woodland.

Bulk-ground electrical resistivity surveys should be less affected by above-ground interference by physically inserting probes into the ground (see [28 Milsom & Eriksen 2011]). Resistivity surveys have been successfully used to

locate unmarked burials in cemeteries (e.g. [29-30 Buck 2003; Matias et al. 2006]), although local variations in soil moisture content, particularly when surveying in dry conditions in heterogeneous ground, affected many surveys by masking target locations (e.g. see [21 Ellwood et al. 1990]. [28 Milsom & Eriksen (2011)] showed obtaining data from areas surrounding graves can be problematic due to inability for probes to penetrate concrete, tarmac or other hard surfaces. Electrical resistivity surveys for clandestine burials of murder victims have also been undertaken with mixed success (see [31-33 Ellwood 1994; Cheetham 2005; Pringle & Jervis 2010]). Long-term monitoring studies of simulated clandestine burials of murder victims have shown electrical resistivity methods should resolve burials, although detection success depends on burial style, soil type and time since burial (see 34 Pringle et al. 2012b). Optimum surveys have also been shown to be undertaken during winter months; in dry conditions numerous non-target anomalies are present due to differential drying of heterogeneous soil (see 34 Pringle et al. 2012b). Simulated studies also evidence that decompositional fluids may be the dominant factor for detecting murder victim clandestine graves (see [34,35] Jervis et al. 2009; Pringle et al. 2012b) which may be retained in grave soil for considerable periods of time post-burial (see [19] Juerges et al. 2010) that is detected electrically.

Ground penetrating radar (GPR) has been used to locate unmarked grave burials in graveyards and cemeteries with varying degrees of success (e.g. [6, 21, 23, 31, 36-41] Kenyon 1977; Ellwood 1990; Bevan 1991; King et al. 1993; Nobes 1999; Powell 2004; Watters & Hunter 2004; Stanger & Roe 2007;

Fiedler et al. 2009; Doolittle & Bellantoni 2010), and indeed of a suspected clandestine burial of a murder victim within a graveyard [42 Ruffell, 2005]. Suggestions by [12 Ruffell et al. 2009] suggest optimum 200 – 400 MHz frequency antennae for unmarked burials. Long-term monitoring studies of simulated clandestine burials of murder victims have again proved useful in determining optimum antennae frequency for detection and effect of local soil type and burial environment (see [34, 43-46 Schultz et al. 2006; Pringle et al. 2018/2012b; Schultz 2008; Schultz & Martin, 2011]). That said, there was wide variation on optimum GPR antennae frequencies for clandestine graves of murder victims, with suggested frequencies commonly varying from 110 MHz up to 800 MHz. There have also been studies which document rapidly-dug grave burials for mass fatalities (19th Century Irish Potato famine ([12 Ruffell et al. 2009]), early 20th Century Spanish Flu victims ([47 Davis et al. 2000]) and animal disease outbreaks [48 Ruffell & Kulesa 2009] respectively which evidence depths of burial significantly shallower than 1.8 m below ground level or bgl. GPR has become the geophysical tool of choice for unmarked graves due to detection success, but may not be suitable in all occasions, for example, where clay-rich and saline soils are present in survey areas where radar waves become rapidly attenuated (see [18,49 Reynolds 2011; Pringle et al. 2012c]). This poses problems in certain countries, for example the UK has soil types which are dominantly clay-rich [50 Chapman 2005]. However some authors (e.g. [25 Nobes, 1999]) have determined low frequency GPR antennae could be used in some clay-rich soils to identify likely burial positions. GPR data processing also requires a good understanding of radar theory, and specialist operators or training of non-specialists; either of which is costly.

170

171 An opportunity arose to assist in the detection of unmarked burials in three

172 geographically spread U.K. graveyards by separate archaeology and clergy

173 approaches. Using these study results and the wider literature, the overall aims

174 of this forensic archaeology geophysical paper are: **Firstly** identify the locations

175 of any unmarked graves and/or burial plots/vaults within the respective survey

176 areas. Identified remains could then be exhumed and re-interred elsewhere by

177 archaeological teams (if necessary). **Secondly** to compare GPR and resistivity

178 geophysical equipment configurations, data acquisition strategies and

179 processing methods to determine best practise for unmarked burial detection in

180 burial grounds. **Thirdly** to provide examples to assist with determining the

181 effect of differing soil type on geophysical surveys and burial detection.

182 **Fourthly** and **finally**, to quantify the variety of burial styles *present in these*

183 *cases, their geophysical responses and comparison to clandestine burials of*

184 *murder victims.*

185

2. Case Study 1: St. James' Church, Newchapel, Staffordshire, UK

2.1. Case study 1: Background

St. James' Church in Newchapel village (SJ 8623 5450) lies ~220 m above sea level on a hill in the north-east of Stoke-on-Trent, UK (Fig. 1). A clay-rich soil overlay the Carboniferous Coal Measures Formation sandstones bedrock geology. However, three boreholes drilled for site investigation (Fig. 1 for location) found the top 2 m bgl comprised predominantly of 'made ground', gravelly clay, occasional brick and coal fragments, with an average moisture content of 16% [51 Fairclough 2008]. A stone chapel was on site by 1573 but was rebuilt in brick in 1766 and 1777, and again in 1878-1915 due to mining subsidence [52 Cramp et al. 2010]. Burial within the churchyard was underway by 1722, although earlier interments may have taken place. The burial ground was periodically extended between the late 18th and early 20th century. In 2004 planning permission was granted for a community hall over part of the graveyard (Fig. 1). An existing plan identified 18 separate grave plots, within the proposed development area, each marked by memorial stone (Fig. 1 and Table 1). It was estimated that these plots represented the burial of up to 68 individuals, interred between 1821 and 1966.

After memorials had been cleared, an archaeological team were on site during removal of ~1.4 m of mechanical soil clearance within the development area. This operation not only revealed presence of several known burials (Fig. 1), but also two unmarked graves (marked A & P in Fig. 1). Geophysicists at Keele

University were subsequently contacted to help identify any additional unmarked burials within the area.

2.2 Case study 1: Geophysical data collection & processing

Upon arrival on site, three of the burials exposed within the survey area were already being archaeologically excavated (Fig. 2). A N-S orientated survey grid was established with 0.5 m spaced lines, avoiding both areas of archaeological excavations and ongoing construction work (Fig. 1). Trial GPR 2D profiles were collected over an exposed burial vault (Figs. 1 and 2) using PulseEKKO™ 1000 equipment and 110 MHz to 900 MHz dominant frequency antennae to determine the optimum antennae for the site. 225 MHz frequency fixed-offset antennae were judged optimal on this site, due to good penetration depths when viewing field data, target graves being resolved, the speed of data collection and best practice recommendations (see [12 Ruffell et al. 2009]). It should be stated, however, that the top 1 m bgl of topsoil had been removed prior to geophysical data acquisition at this site. The survey grid was surveyed (Fig. 2a) using a 150 ns time window, 0.1 m trace interval and 32 constant signal stacks. This took ~8 h to acquire. Any identified targets were marked for intrusive archaeological investigation. A Common-Mid Point (CMP) survey obtained onsite a 0.07 m/ns average site velocity to convert 2D GPR profiles from two-way time to depth following standard methodologies (see [28 Milsom & Eriksen, 2011]).

Once the 2D GPR profiles were acquired, they were downloaded and imported into REFLEX-Win™ v.3.0 processing software. For each 2D profile, a series of

sequential data processing steps were used. These were: (1) Subtract mean ('de-wow' to remove any positive or negative bias of the trace; (2) Move start-time to uniform time, based on common reflector which allowed all features of uniform depth below ground-level to appear uniform in profiles; (3) 1D Bandpass (Butterworth) filter to remove the upper/lower extents of frequency histogram; (4) 2D filter back-ground removal to remove average from entire trace, removing interfering 'ringing' created during the bandpass filter stage; (5) Gain Energy decay (SEC) function applied to enhance late arrival wave amplitudes; (6) Migration (Stolt) to collapse hyperbolae to discrete focus points; (7) Horizontal time-slice generation to collapse specific time region across all profiles to create a 'map-view' of total amplitude over time/depth domains and finally; (8) Amplitude data exported as xyz data file into 0.25 m (X) x 0.025 m (Y) spaced .xyz file for graphical presentation. Note 2D profiles were interpreted after stage 5. Absolute amplitude time-depth slices were generated at specified depth regions to assess whether they were likely candidate for burials based upon their orientation, dimensions and depth bgl. Finally the time-slices were imported into Generic Mapping Tools (GMT) software for visualisation purposes.

A small, twin-probe (0.5 m fixed-offset) bulk-ground resistivity survey was also collected over a small area (Fig. 1) for comparison with the GPR data, using a Geoscan TM RM15-D resistivity meter and PA20 probe-array (Fig. 2b). The mobile 0.1 m long stainless steel electrode probes were separated by 0.5 m, whilst the remote probes were placed 1 m apart at a distance of at 10 m from the survey position following best practice procedures [28 Milsom & Eriksen,

2011]. For each 0.25 m spaced resistivity measurement on 0.5 m spaced profile lines, the mobile probes were inserted ~0.05 m into the ground. The data logger automatically collected and recorded resistivity measurements at each sample position. The RM15 survey took ~1 h to acquire.

Once the resistivity data were downloaded from the resistivity meter, converted into x,y,z format data and x,y raw positions moved, where appropriate, before being processed in Generic Mapping Tools (GMT) software [53 Wessel & Smith, 1998], a series of sequential data processing steps were used. These were: (1) Conversion, spatially-corrected data to XYZ in GMT (where applicable); (2) Minimum curvature gridding algorithm was used to interpolate each dataset to a cell size of 0.125 m x 0.125 m for visualisation; (3) Long-wavelength trends were then removed by fitting a cubic surface to grid and subtracting from surface data, to allow smaller, grave-sized features to be more easily identified; (4) Normalisation by dividing datasets by their SD Z value created grid with mean Z of ~0 and SD of ~1 allowing dataset comparison and finally; (5) All processed map-view datasets were then combined with site satellite images, archaeological and engineering information within CorelDRAW™ v.12 graphical software.

2.3 Case study 1: Geophysical results

Multiple discrete hyperbolic reflectors were observed on 2D GPR profiles at 10 – 40 ns that were ~0.4 – 2 m depth bgl (for example, see Fig. 3). There were a number of different burial styles interpreted within the graveyard, based on

anomalies characters and depths (Fig. 3). Identified hyperbolae spatial positions and time-depths were graphically marked on the study mapview plan before being unmarked burials and vault positions were interpreted. Radar signal amplitude anomaly positions in the horizontal time-slices were also compared to 2D profiles and grave marker positions (Fig. 4). Time-slices were used to confirm the approximate depths of burials based on the presence (or lack thereof) of associated features at set time-depth slices, with all amplitude anomalies showing as east-west orientated rectangular anomalies. These features were ~1-2 m long, correlating with the approximate dimensions of isolated adult human burials (Fig. 4).

The raw resistivity dataset had 73/88/204.7 $\Omega\cdot\text{m}$ (minimum/average/maximum) values recorded with a 14.4 SD. There was a relatively high 2 m x 2 m anomaly, with respect to lower background values, that was correlated to the double G burial vault (Fig. 5). The highest relative resistivity values were at vault edges, suggesting low porosity construction material (e.g. brick).

Combining all the geophysical results, it was suggested that there were an extra ten unmarked burials that were not previously identified (Fig. 6). There was also observed two main burial orientations, some being concordant with the present church footprint but the majority at ~20° clockwise angle different from these (Fig. 6).

2.4 Case Study 1: Archaeology excavations

Archaeological excavation subsequently confirmed these results (Fig. 7 and Table 2). Seven coffined burials were exhumed from three different burial environments within the graveyard: three from a single vault, three from brick-lined graves and one (A) from an unmarked earth-cut grave (Table 2). Vaults are brick-built, sub-ground chambers accessed via a discrete surface entrance that was sealed between interments [54 Stock 1998]. They are typically of sufficient area to accommodate two burials positioned side by side and usually in layers [55-56 Litten 1992; Buteux & Cherrington 2006]. In contrast, brick-lined (and indeed earth-cut) graves are wide enough in plan to take only a single coffin (and are often coffin-shaped), although they can be cut deep enough to take a stack of several interments, each separated by a stone slab.

The coffins, although in varying states of decay, all featured copper-alloy fittings, principally *deposita* (breastplates), but also grips (handles), grip plates, escutheons and carrying rings [52 Cramp et al. 2010]. Coffin ornamentation with such mass-produced items was a common practice during the 19th and early 20th centuries [55 Litten, 1992].

The excavated earth-cut grave (A) featured a single coffin placed directly into the ground. The brick-lined graves accommodated either one or two burials; the base of the single-interment (Eb) comprised un-mortared flagstones, whereas two stacked burials (Ea) used a suspended sandstone floor to separate the coffins (Fig. 7). An unusual glass viewing face panel was recovered from one coffin remains (CF200). The brick burial vault (C) contained four interments laid in pairs on two levels, separated by sandstone

337 slab floor. The occupants belonged to one family and recorded on the
338 monument that marked the burial site. The monument also commemorates an
339 additional three individuals who were not present within the vault, suggesting
340 that limited space was managed through intermittent removal of remains.
341

3. Case Study 2: St. Luke's, Endon, Staffordshire, UK.

3.1 Case study 2: Background

St. Luke's Church in Endon village (SJ 9281 5380) lies ~190 m above sea level on a hill 10 km north-east of Stoke-on-Trent, U.K. (Fig. 8). A coarse sandy soil containing predominantly sandstone pebbles overlay the Triassic Hawkesmoor Formation sandstones and conglomerate bedrock geology. The Audley family established a chapel in the 13th century [57 Tringham 1996], although the exact location and when it fell into disuse is unknown [58 Speake 1974]. The present church was constructed between 1719 and 1721 [58 Speake 1974], with periodic alterations in 1830, 1870, 1970 and 1981.

The first recorded burial was in March 1731; by 1830 part of the churchyard had been turned into a garden with landscaping at the western end shortly after [58 Speake 1974]. The graveyard was extended in 1898 [59 Kelly 1921] and it is likely that some burial relocation and memorial clearance took place. Additional monuments were removed in the mid 1970s [60 Sutherland 2012]. Planning permission for single-storey extensions to the west and north was granted in 2007. The construction of both buildings would impact upon adjacent burials, some of which had headstones and Grade II Listed chest tombs (Fig. 8). The northern side church extension was geophysically surveyed on the 20th and 21st October 2010. The west extension area was not surveyed due to the presence of steps and hard paths (Fig. 8).

3.2 Case study 2: Geophysical data collection & processing

Observed grave stones were all E-W oriented as is common for UK burials [55 Litten 1992]. A N-S orientated survey grid was therefore established with 0.5 m spaced lines (Fig. 8). Trial GPR 2D profiles were collected over a known burial position using available PulseEKKO™ 1000 equipment and 110 MHz to 900 MHz dominant frequency antennae to determine the optimum antennae for the site. 225 MHz frequency fixed-offset antennae were judged optimal on this site as per case study 1 recommendations. The full survey grid was then surveyed (Fig. 9) using a 80 ns time window, 0.1 m trace intervals and 32 constant signal stacks. A CMP survey was also obtained onsite to gain a 0.12 m/ns average site velocity to convert 2D GPR profiles from two-way time to depth. The GPR survey took ~12 h to acquire. Due to the potential of resistivity surveys to detect burials from case study 1, the full survey area was acquired using the Geoscan™ RM15-D resistivity meter and PA20 probe-array. Sample positions were acquired using a twin-probe at both 0.5 m and 1 m fixed-offset spacings (Fig. 9b), using the same methodology as case study 1. Contact resistances were very high and needed remote probe separations to be 1.5+ m, a number of measurements could still not be recorded. The RM15 survey took ~8 h to acquire.

Both GPR and resistivity dataset processing were the same as for case study 1. All processed map-view datasets were combined with site satellite images, archaeological and other information within CorelDRAW™ v.12 graphical software.

3.3 Case study 2: Geophysical results

Multiple discrete hyperbolic reflectors were observed on 2D GPR profiles at 8 – 20 ns that were ~0.6 – 1.8 m depth bgl (for example, see Fig. 10). Most burial positions seemed to be earth-cut graves, based on anomalies characters, depths and comparisons to case study 1 (*cf.* Figs. 3 and 10). Identified hyperbolae spatial positions and time-depths were graphically marked on the study mapview plan. Radar signal amplitude anomaly positions in horizontal time-slices were also compared to 2D profiles and grave marker positions (Fig. 11). Time-slices were used to confirm the approximate depths of burials based on the presence (or lack thereof) of associated features at time-depth slices, with amplitude anomalies showing as east-west orientated rectangular anomalies. These features were ~1-2 m long, correlating with approximate dimensions of isolated adult burials (Fig. 11).

The raw 0.5 m fixed-offset probe spacing resistivity dataset had 26/89.9/204.7 $\Omega\cdot\text{m}$ (minimum/average/maximum) values recorded with a 37.9 Standard Deviation (SD). The raw 1.0 m fixed-offset probe spacing resistivity dataset had -91.7/71.8/204.5 $\Omega\cdot\text{m}$ (min./av./max.) values recorded with a 56.6 SD. 43% of the survey area was not able to be recorded using the 1 m separated (fixed-offset) mobile probes so results have not been shown here. The processed 0.5 m spaced resistivity dataset is shown in Figure 12. There were not clear burial-sized anomalies present in this dataset, with clear relative high resistivity

anomalies correlating with tree positions and a cluster of burials at the east of the survey area (Fig. 12).

Combining the geophysical results with the surviving surveyed headstone data, it was suggested that there were an extra nineteen unmarked burials that were not previously identified (Fig. 13).

3.4 Case study 2: Archaeology excavations

An archaeological evaluation was undertaken within the western extension area (Fig. 14). This showed fifteen earth-cut graves, two of which (G03 & G10) were intercut. Four (G01/G02 and G05/G08) were stacked in pairs, perhaps indicating family plots (Fig. 14 and Table 3). Average burial depth was 1 m bgl (minimum burial depth was 0.80m bgl, the maximum 1.25m bgl) although this was ~1 m below present ground level. All burials were confined, although both caskets and skeletal remains were typically in poor condition; five showed evidence of post-burial disturbance. Copper-alloy and iron coffin furniture were present in many cases, but were generally poorly preserved. Conversely, three graves (G03, G05 and G14) included well-preserved items of clothing and footwear.

4. Case Study 3: St. John of Jerusalem, Hackney, London, UK.

4.1 Case study 3: Background

St. John of Jerusalem church in South Hackney (TQ 3555 8455) lies ~15 m above sea level around 10 km north-east of the centre of London, UK (Fig. 15). The Hackney Gravel Member alluvium soils overlay the Eocene London Clay Formation bedrock geology. The present stone church was completed in 1848 and the graveyard was filled by 1868, the stone spire replaced by copper after bomb damage during WW2 [61 Taylor 2002]. Grave stones from significant areas of the graveyard were removed at some period during the 1960s (Rev. A. Wilson, *pers. comm.*), leaving large areas of the graveyard unmarked. However, rectangular-shaped depressions were observed in the graveyard, together with some exposed snapped off head stone bases and remaining stone tombs which may or may not be *in situ* (Fig. 16). The church vicar was planning for an extension on the west of the church over part of the graveyard (Area A) and also wished to know the location of unmarked burials in another area of the graveyard (Area B) (see Fig. 15). The site was topographically and geophysically surveyed on the 9th – 10 September 2010.

4.2 Case study 3: Geophysical data collection & processing

Remaining grave stones and visible snapped head stone bases (Fig. 16b) were topographically surveyed within both survey areas. A N-S orientated survey grid was established over both survey areas with 0.5 m –spaced lines (Fig. 16),

avoiding trees and densely vegetated borders (Fig. 15). Trial GPR 2D profiles were collected over suspected burial rectangular surface depressions using PulseEKKO™ equipment and 110 MHz to 900 MHz dominant frequency fixed-offset antennae to determine the optimum antennae for both areas; 450 MHz dominant frequency antennae were determined to be optimal in Site A whereas 225 MHz was determined to be optimal in Site B as per case study 1 recommendations. Survey grid A was surveyed (Fig. 16a) by the 450 MHz antennae using a 80 ns time window, 0.05 m trace intervals and 32 constant signal stacks. Survey grid B was surveyed (Fig. 16b) by the 225 MHz antennae using a 100 ns time window, 0.1 m trace intervals and 32 constant signal stacks. A CMP survey was also obtained onsite to gain a 0.1 m/ns average site velocity to convert 2D GPR profiles from two-way time to depth. The GPR survey took ~14 h to acquire. Both survey grids were also surveyed using the Geoscan™ RM15-D resistivity meter and PA20 probe-array. Sample positions were again acquired using a twin-probe at both 0.5 m and 1 m fixed-offset spacings (Fig. 16b), using the same methodology as case study 2. The RM15 survey took ~10 h to acquire. In the west part of Area B, a number of animal burrows were present (including one ~0.5 m x 0.25 m); an urban fox was also observed entering.

Both GPR and resistivity dataset processing were the same as for case study 1. All processed map-view datasets were combined with site satellite images, archaeological and other information within CorelDRAW™ v.12 graphical software.

4.3 Case study 3: Geophysical results

In area A, multiple discrete hyperbolic reflectors were observed in 2D profiles at 5 – 20 ns that were ~0.2 – 1.0 m depth bgl (for example, see Fig. 17a). In area B, multiple discrete hyperbolic reflectors were also observed in 2D profiles at 10 – 40 ns that were ~0.5 – 1.5 m depth bgl (for example, see Fig. 17b). Most burial positions seemed to be isolated earth-cut graves, based on anomalies characters, depths and comparisons to case study 1 although one does indicate multiple grave occupants (*cf.* Figs. 3 and 17). Identified hyperbolae spatial positions and time-depths were graphically marked on the study mapview plan.

Radar signal amplitude anomaly positions in horizontal time-slices were also compared to 2D profiles and grave marker positions (Fig. 18). Time-slices were used to confirm the approximate depths of burials based on presence (or lack thereof) of associated features at time-depth slices, with amplitude anomalies showing as northeast-southwest orientated rectangular anomalies. These features were ~1-2 m long, correlating with approximate dimensions of isolated adult burials (Fig. 18).

For area A the raw 0.5 m fixed-offset probe spacing resistivity dataset had 74/101/178 $\Omega\cdot\text{m}$ (minimum/average/maximum) values recorded with a 11.8 Standard Deviation (SD). The raw 1.0 m fixed-offset probe spacing resistivity dataset had 55.6/73.1/200 $\Omega\cdot\text{m}$ (min./av./max.) values recorded with a 7.2 SD. For area B the raw 0.5 m fixed-offset probe spacing resistivity dataset had

49/114.7/204.7 Ω .m (minimum/average/maximum) values recorded with a 29.8 Standard Deviation (SD). The raw 1.0 m fixed-offset probe spacing resistivity dataset had -1.4/68.6/204.5 Ω .m (min./av./max.) values recorded with a 11.5 SD. The processed 0.5 m and 1 m probe-spaced resistivity datasets are shown in Figures 19 and 20 respectively. There were numerous burial-sized anomalies present in these datasets; note the large relatively high resistivity anomaly area in the south-west of Area B could be correlated with the observed fox den burrow.

In Area A the geophysical results suggested there were thirteen unmarked burials (Fig. 21). In Area B four burials were located by surveying snapped off headstones, the geophysical survey here additionally suggested that there were an extra forty-six unmarked burials that were not previously identified (Fig. 21).

4.4 Case study 3: Geophysical validation

Unfortunately there was no subsequent archaeological excavation to confirm the geophysical survey results. However, part of the graveyard to the south of the church ($\sim 200 \text{ m}^2$) had 21 grave markers intact, orientated NE-SW, predominantly isolated (presumably) earth-cut graves with two family vaults containing four individuals. The geophysical survey results, which has interpreted predominantly earth-cut grave, would seem to confirm a similar style to the observed intact grave markers.

5. Discussion

This section is organised to answer and discuss the study objectives in sequential order.

5.1 Identify the locations of any unmarked graves and/or burial plots/vaults within the respective survey areas. Identified remains could then be exhumed and re-interred elsewhere by archaeological teams (if necessary).

All three case studies evidenced near-surface geophysical methods could detect the locations of both unmarked graves and vaults, with case studies 1 and 2 being subsequently archaeologically excavated. The distribution of both geophysically interpreted and archaeologically excavated graves were not uniformly spatially distributed or indeed their locations predicted, for example, Area A in case study 3 had surprisingly few graves (Fig. 21), despite it's relative proximity to the church, whereas the archaeologically excavated area in case study 2 which was also close to its church had a relatively dense clustering of graves at various depths bgl, with some graves even cross-cutting each other at different depths (see Fig. 14). Most excavated grave coffins also had numerous copper-alloy fittings which may or may not be magnetic and/or conductive but others (e.g. [21,22 Ellwood 1990; Witten et al. 2001]) have had mixed success using magnetics as a burial detection tool. Geophysical anomalies in the case studies shown here (in map view) could allow their relative orientations to be established, in case study 1 it could be argued that grave ages could be approximately dated by alignment to the different church

building orientations that were built onsite during different time periods (Fig. 6). All geophysical anomalies were orientated perpendicular to the church building footprint (c.f. Figs. 6, 13 and 21). However, in case study 1 two known burial positions were not able to be imaged in the geophysical data, therefore suggesting that these methods may not find all unmarked burials.

Grave markers in burial grounds, if present, will not necessarily be accurate in marking burial positions as other authors have evidenced (see [6,55] Fiedler et al. 2009; Litten 1992); headstones have been rotated or indeed moved to make space or for other unknown reasons. All the case studies detailed here found more unmarked burials than could be discerned by grave markers and respective parish records alone. Subsequent archaeological excavations (Tables 2-3) also found named individuals where expected as well as extra unnamed individuals and missing individuals (although older burials may have completely fragmented) which gives less confidence in burial records.

5.2 Compare GPR and resistivity geophysical equipment configurations and data acquisition strategies and processing methods to determine best practise for unmarked burial detection in burial grounds.

GPR 225 MHz dominant frequency antennae were determined to be optimal in all three case studies, although note case study 1 had the top 1 m bgl of soil removed before surveying and Area A of case study 3 had 450 MHz dominant frequency antennae judged to be optimal. This is broadly consistent with other authors on unmarked burial detection (e.g. [6,12 Fiedler et al. (2009); Ruffell et

al. 2009] who found 250 MHz - 500 MHz frequency antennae were optimal, although [29 Buck 2003] found 800 MHz optimal.

Electrical resistivity fixed-offset probe separations of both 0.5 m (common in forensic geophysical surveys, e.g. [32 Cheetham 2005]) and 1 m were trialled in case studies 2 and 3; in case study 3 it could be argued that the 1 m probe separation data were better at locating unmarked graves (*cf.* Figs. 18 and 19). However, note the 1 m probe separation dataset from case study 2 were not usable. This was probably due to the soil type (see section 5.3). As penetration depths are typically 1-2 times the probe separation (see [28] Milsom & Eriksen, 2011) the 1 m dataset will penetrate further bgl and would therefore be less affected by heterogeneous material in the very top surface. An unforeseen outcome using electrical resistivity surveys was that a number of unmarked burials were located by the instrument probes themselves, encountering grassed-over horizontal stone slabs laid on top of the graves (see Fig 22); particularly in case studies 2 and 3.

For data acquisition strategies, from this paper and the wider literature (e.g. [12,34, 42, 43,46 Schultz et al. 2006; Ruffell et al. 2009; Schultz & Martin, 2011; Pringle et al. 2012a]) it is judged critical to undertake trial 2D profile data collection over known burial targets (if known) prior to full survey data collection. Every survey site is unique with different soil types, local depositional environment (see section 5.3), burial history, etc.; trials should allow optimum equipment configurations to be determined. Most unmarked burials in this papers Christian burial grounds were east-west orientated albeit

with some variation (see Figs. 6, 13 and 21); all were orientated orthogonally to their respective church building orientation so this needs to be borne in mind when orientating survey lines (which should usually be north-south orientated). This paper and others (e.g. [25, 42 Nobes 1999; Ruffell et al. 2009]) have also detailed 0.5 m spaced survey lines should successfully detect unmarked burials, at least of adults. Soil type is also important for technique selection as section 5.3 details. Other authors' electrically monitoring simulated clandestine burials of murder victims (e.g. [34, 35 Pringle et al. 2012b, Jervis et al. 2009]) have also shown significant temporal variations; winter surveys are suggested to be optimal for electrical resistivity surveys when less non-target anomalies are present.

GPR data processing showed careful utilisation of bandpass filtering, coupled with background removal as other authors (e.g. [25] Nobes 1999) have shown and gain functions significantly improved the image quality of 2D profiles. GPR horizontal time-slices were also found to be useful to correlate targets with resistivity datasets as [41 Doolittle & Bellantoni (2010)] observed, but here usable horizontal time-slices required significant data processing time.

Electrical resistivity data processing requires data de-spiking as a minimum, with site detrending in 3D to remove long wavelength trends and revealing anomalous positions deemed important as forensic electrical resistivity work has shown (e.g. see [17,33 Pringle et al. 2012a; Pringle & Jervis 2010]).

5.3 Provide examples to assist with determining the effect of differing soil type on geophysical surveys and burial detection.

637
638 GPR has been judged optimal for unmarked graves (e.g. [17, 25, 42 Nobes
639 1999; Ruffell et al. 2005]) and clandestine murder victims (e.g. [34,43,44
640 Schultz et al 2006; Schultz 2008; Pringle et al. 2012b]) burial detection
641 respectively in sandy soils. In these soils, bulk electrical resistivity has also
642 been suggested to be highly useful for unmarked graves (e.g. [29-30 Buck
643 2003; Matias et al. 2006]) and clandestine murder victims (e.g. [32, 33
644 Cheetham 2005; Pringle & Jervis 2010]) burial detection respectively. In clay-
645 rich soils GPR is generally not optimal for unmarked graves (e.g. [25 Nobes
646 1999]) and clandestine murder victims ([e.g. 17, 33 Pringle & Jervis 2010;
647 Pringle et al. 2012a) burial detection respectively. However in clay-rich soils
648 bulk electrical resistivity is judged to be optimal for unmarked graves ([e.g. 25
649 Nobes 1999]) and clandestine murder victims (e.g. [33 Pringle & Jervis 2010])
650 burials respectively. In this study where soils were typically black earths (case
651 study 3), then again both GPR and bulk electrical resistivity surveys were
652 judged to be optimal for unmarked grave burial detection. However, where
653 soils were relatively coarse with pebbles (case study 2) then GPR was judged
654 optimal whilst resistivity surveys were not recommended. Little published work
655 has been undertaken on detection of unmarked burials in coastal/saline soils
656 although a simulated coastal clandestine burial of a murder victim suggested
657 that magnetics and resistivity may be optimal in such environments [49 Pringle
658 et al. 2012c]. Lastly where grave soils have been repeatedly re-used (e.g. case
659 study 1) and highly variable within the same burial ground as others have found
660 (e.g. [25 Nobes 1999]), they are more of a 'made ground' soil and it can be
661 difficult to resolve burials; happily in case study 1 most graves were brick-lined

and these could easily be resolved in 2D GPR profiles (e.g. see Fig. 3). Indeed it is suggested that the predominance of these brick-lined earth-cut graves may have been due to this difficult ground encountered (see Fig. 2 and [52] Cramp et al. 2010). Wooden coffin (and indeed individuals contained within) preservation was highly varied (from good to poor preservation) on the same site and from similar burial ages (Tables 4 and 5), for reasons that are presently unclear.

The local depositional environment can also be important, deciduous trees were present in all three case studies and indeed are common in UK graveyards [55 Litten 1992]; apart from those areas not being able to be geophysically surveyed, tree roots can interfere with successful identification of buried anomalies, either directly by generating shallow GPR reflection events (see Fig. 17a) or by gaining relative high resistance anomalies in proximity to trees (see Fig. 19) which other authors (see, e.g. [62] Jones et al. 2010) have attributed to reduced soil moisture content. Near-surface animal burrows were also a considerable issue in Area B in case study 3, in this area GPR was deemed optimal over resistivity methods because of the presence of these burrows.

5.4 Quantify the variety of U.K. burial styles present in these cases, their geophysical responses and comparison to clandestine burials of murder victims

Case study 1 and 2 evidenced burials were interred in wooden coffins in earth-cut graves (e.g Fig. 14) to be present that were typical of UK graveyards during

the 19th – early 20th century [55 Litten 1992]; however subsequent
 archaeological excavations found a variety of other burial styles, for example,
 brick-lined graves were predominant in case study 1 (Fig. 7 and Table 2), which
 also featured a brick-built family vault with individuals interred side-by-side in at
 least two layers (Fig. 6). Multiple burials were also observed, both in the same
 grave position and also in case study 2 being cross-cut at different depths bgl
 (Fig. 14). These varieties in burial style have been schematically summarised
 in Figure 22 and their respective geophysical responses summarised in Table
 4. Isolated earth-cut graves (Fig. 22a) can be observed from all case studies,
 defined as an obvious $\frac{1}{2}$ hyperbolic GPR reflection event on 2D profiles (see
 Fig. 10) and isolated relative high/low rectangular resistivity anomalies (Fig. 20).
 Multiple occupancy earth-cut graves (Fig. 22b) were also observed from all
 case studies, defined as either vertically or slightly off-set obvious $\frac{1}{2}$ hyperbolic
 GPR reflection event on 2D profiles (see Fig. 17b). Isolated brick-lined graves
 (Fig. 22c) were observed from case studies 1 and 3, defined as near-surface
 narrow GPR reflection events either side of a clear $\frac{1}{2}$ hyperbolic reflection
 event (Fig. 10b). Multiple brick-lined & top slab graves (Fig. 22d) and vaults
 (Fig. 22e) were observed in case study 1, defined as near-surface narrow
 reflection events either side of multiple clear $\frac{1}{2}$ hyperbolic reflection events (Fig.
 10). Electrical resistivity anomalies for all burial styles were rectangular (in
 mapview), with multiple occupancy graves generally being either larger and/or
 stronger negative/positive anomalies with respect to background values.

Generally isolated and multiple earth-cut graves were fairly straightforward to
 distinguish in the GPR data by clear $\frac{1}{2}$ hyperbolic reflection events on 2D

712 profiles, and indeed differentiate with brick-lined and top slabbed graves which
713 had narrow reflection events on 2D GPR profiles from the brick lining. It was
714 harder to differentiate burial styles in map view using either GPR time-slices
715 and/or electrical resistivity data which both had rectangular high amplitude
716 anomalies for all burial styles. One unknown was burial age, it would be
717 expected that older burials would be harder to detect due to being unmarked,
718 soil compaction and target degradation so this may be why some burials were
719 undetected. It was also unknown if some geophysical anomalies represented a
720 single interment or if multiple occupancies were present if there was no
721 archaeological excavations undertaken (such as in case study 3). Known burial
722 markers were not always reliable indicators as already discussed.

723
724 The physical characteristics of graves in graveyards and cemeteries are quite
725 different from isolated and indeed mass clandestine burials of murder or animal
726 victims (see [17] Pringle et al. 2012a) although others (e.g. [63] Mellett 1992)
727 have suggested they could be used as analogues. Human burials in
728 graveyards and cemeteries are commonly buried much deeper below ground
729 level (Fig. 22) and, as well as remains, may contain embalming fluid and have
730 coffins with varying contents and indeed coffin furniture (see [55, 64] Litten,
731 1992; Ruffell & McKinley 2008). Average burial depths of discovered
732 clandestine graves of murder victims are ~0.5 m bgl [17 Pringle et al. 2012a]
733 whereas typically isolated grave burials in graveyards and cemeteries (Fig. 22)
734 are typically ~1.8 m bgl (see [65 Cox & Hunter 2005]). Note rapidly-dug
735 unmarked burials (e.g. [23,47 Ruffell et al. 2009; Davis et al. 2000] may be
736 more analogous to clandestine burials of murder victims. [66 Vaughan (1986)]

point out that graves are difficult to detect due to being typically old, buried deep and contain limited skeletal remains. The schematic comparison Figure 23 to compare unmarked burials versus clandestine graves of murder victims styles is instructive but a generalisation, there will be site specific variables, including soil type and local depositional environment [17,68 Harrison & Donnelly 2009; Pringle et al. 2012a], specific age of burials, presumed burial style variability and decomposition rates, and to make things even more complicated, and as shown here and by others (e.g. 25 Nobes 1999) some of these variables have been even documented to vary within the same burial site.

6. Conclusions

Combined GPR and electrical resistivity geophysical methods were used successfully in identifying unmarked graves and burial vault positions in three UK case studies. Subsequent archaeological excavations of two case studies evidenced these successes as well as documenting a surprising variety of burial styles, from earth-cut isolated graves, brick-lined graves, to cross-cut graves, multiple occupancy and horizontally stacked family vaults. Coffin contents also varied, including missing/extra individuals when compared to burial records and various items of coffin furniture. Grave and vault markers also did not always indicate the presence, location or character of burials. Parish records should therefore be used with caution.

225 MHz dominant frequency GPR antennae were deemed optimal in these surveys due to successful detection of burial positions, penetration depths bgl and acquisition rates. 1 m (fixed offset) probe separations were recommended for electrical resistivity surveys, but resistivity surveys should be used with caution on sites with very coarse grained soils, soil type being evidenced here as a major factor. One burial ground also showed significant re-use and was termed here 'made ground' which would make interpretation of geophysical data difficult for non-experts. Careful data processing is essential; resistivity data should be 3D detrended to resolve geophysical anomalies. Areas with tree roots and animal burrows were problematic.

Further studies from other graveyards, with contrasting soil types and burial ages, would provide a greater understanding of geophysical surveys to detect such forensic targets. It would also be instructive to collect GPR, magnetics and bulk ground electrical resistivity datasets in several graveyards and cemeteries with contrasting soil types over marked burials with known individuals and burial dates. This would allow further clarification of optimum geophysical equipment for soils to be determined and also to gain important temporal information that is currently lacking in the literature. It is recommended that geophysical surveying should be undertaken before site development work is initiated, particularly in case study 1 where some parts of the graveyard could not be surveyed and 1 m of top soil was removed prior to surveying. Forensic geophysical surveys in cemeteries and graveyards will become increasingly important to undertake to not only detect unmarked burials but also to find where no burials are present due to the current chronic lack of burial space in the UK.

789 **7. Role of the funding source**

790

791 There was no involvement of any funding sources with this project.

792

793 **8. Acknowledgements**

794 The authors would like to thank Mr Richard Cramp and Ms Zoe Sutherland of
795 Stoke-on-Trent Archaeology Service for their work on case studies 1 and 2.

796 Kristopher Wisniewski and David Kitley are thanked for case studies 1 and 2
797 field assistance. Oliver Good and Sam Evans are thanked for case study 2
798 field assistance. Claire Holland is thanked for case study 3 field assistance.

799 Two anonymous reviewers greatly improved the manuscript.

800

9. References

[1] Environment Agency, Science project: potential groundwater pollutants from cemeteries, 2004. Available online: <http://publications.environment-agency.gov.uk/pdf/SCHO1204BIKS-e-e.pdf>. Last accessed 10th July 2013.

[2] Ministry of Justice, Burial law & policy in the 21st Century: The way forward. Government response to the consultation carried out by the Home Office/DCA. (2006) <http://www.justice.gov.uk/publications/docs/burial-law-policy.pdf> Last Accessed: 27th August 2013.

[3] Ministry of Justice 2006. Burial Law and Policy in the 21st Century: The Need for a Sensitive and Sustainable Approach. Available online: https://www.gov.uk/government/uploads/system/uploads/attachment_data/file/162865/burial_grounds_web_whole_plus_bookmarks.pdf.pdf. Last accessed: 10th July 2013.

[4] K-H. Jim, M.L. Hall, A. Hart, S.J.T. Pollard, A survey of green burial sites in England and Wales and an assessment of the feasibility of a groundwater vulnerability tool, Environ. Tech. 29 (2008) 1-12.

[5] J.H. Rumble, Giving something back: a case study of woodland burial and human experience at Barton Glebe, Unpublished PhD Thesis, Durham University, 2010. Accessible online at: <http://etheses.dur.ac.uk/679/>. Last accessed: 10th July 2013.

826

827 [6] S. Fiedler, B. Illich, J. Berger, M. Graw, The effectiveness of ground-
828 penetrating radar surveys in the location of unmarked burial sites in modern
829 cemeteries, *J. App. Geophys.* 68 (2009) 380–385.

830

831 [7] D.W. Owsley, Techniques for locating burials, with emphasis on the probe,
832 *J. Forensic Sci.* 40 (1995) 735–740.

833

834 [8] G.M. Brilis C.L. Gerlach, R.J. van Waasbergen, Remote sensing tools assist
835 in environmental forensics, Part I digital tools—traditional methods, *Environ.*
836 *Forensic* 1 (2000a) 63–67.

837

838 [9] G.M. Brilis, R.J. van Waasbergen, P.M. Stokely, C.L. Gerlach, Remote
839 sensing tools assist in environmental forensics, Part II digital tools, *Environ.*
840 *Forensic* 1 (2000b) 1–7.

841

842 [10] D.J. Dickinson, The aerial use of an infrared camera in a police search for
843 the body of a missing person in New Zealand. *J. For. Sci. Soc.* 16 (1976) 205–
844 211.

845

846 [11] M. Statheropoulos, A. Agapiou, E. Zorba, K. Mikedi, S. Karma, G.C. Pallis,
847 C. Eliopoulos, C. Spiliopoulou, Combined chemical and optical methods for
848 monitoring the early decay stages of surrogate human models, *For. Sci. Int.* 210
849 (2011) 154-163.

850

[12] A. Ruffell, A. McCabe, C. Donnelly, B. Sloan, Location and assessment of an historic (150–160 years old) mass grave using geographic and ground penetrating radar investigation, NW Ireland, J. Forensic Sci. 54 (2009) 382–394.

[13] A. Ruffell, J. McKinley, Forensic geomorphology. Geomorphology (2014) <http://dx.doi.org/10.1016/j.geomorph.2013.12.020>

[14] E.W. Killam, The Detection of Human Remains, Charles C Thomas Pubs., Springfield, IL, 2004, 268pp.

[15] T.L. Dupras, J.J. Schultz, S.M. Wheeler, L.J. Williams, Forensic recovery of human remains, CRC Press, Boca Raton, FL, 2006, 232pp.

[16] D.O. Larson, A.A. Vass, M. Wise, Advanced scientific methods and procedures in the forensic investigation of clandestine graves, J. Contemp. Crim. Just. 27 (2011) 149–182.

[17] J.K. Pringle, A. Ruffell, J.R. Jervis, L. Donnelly, J. McKinley, J. Hansen, R. Morgan, D. Pirrie, M. Harrison, The use of geoscience methods for terrestrial forensic searches, Earth Sci. Rev. 114 (2012a) 108–123.

[18] J.M. Reynolds, An introduction to applied and environmental geophysics, 2nd ed., John Wiley & Sons, 2011, 681pp.

- 875 [19] A. Juerges, J.K. Pringle, J.R. Jervis, P. Masters, Comparisons of magnetic
876 and electrical resistivity surveys over simulated clandestine graves in
877 contrasting burial environments, *Near Surf. Geophys.* 8 (2010) 529-539.
878
- 879 [20] N. Linford N, Magnetic ghosts: mineral magnetic measurements on Roman
880 and Anglo-Saxon graves, *Arch. Prosp.* 11 (2004) 167–180.
881
- 882 [21] B.B. Ellwood, Electrical resistivity surveys in two historical cemeteries in
883 northeast Texas: a method for delineating unidentified burial shafts, *Hist. Arch.*
884 24 (1990) 91–98.
885
- 886 [22] A. Witten, R. Brooks, T. Fenner, The Tulsa Race Riot of 1921: a
887 geophysical study to locate a mass grave, *Leading Edge* 20 (2001) 655–660.
888
- 889 [23] R. Stanger, D. Roe, D. Geophysical surveys at the West End Cemetery,
890 Townsville: an application of three techniques, *Aust. Archaeo.* 65 (2007) 44–50.
891
- 892 [24] B. Frohlich, W.J. Lancaster, Electromagnetic surveying in current Middle
893 Eastern archaeology – application and evaluation, *Geophys.* 51 (1986) 1414-
894 1425.
895
- 896 [25] D.C. Nobes, Geophysical surveys of burial sites: a case study of the Oaro
897 Urupa site, *Geophys.* 64 (1999) 357–367.
898

- 899 [26] D.P. Bigman, The use of electromagnetic induction in locating graves and
900 mapping cemeteries: an example from Native North America, *Arch. Prosp.* 19
901 (2012) 31-39.
- 902
- 903 [27] D.C. Nobes, The search for “Yvonne”: a case example of the delineation of
904 a grave using near-surface geophysical methods. *J. For. Sci.* 45 (2000) 715–
905 721.
- 906
- 907 [28] J. Milsom, A. Eriksen, *Field Geophysics*, 4th ed., John Wiley & Sons, 2011.
- 908
- 909 [29] S.C. Buck, Searching for graves using geophysical technology: field tests
910 with ground penetrating radar, magnetometry and electrical resistivity, *J.*
911 *Forensic Sci.* 48 (2003) 5–11.
- 912
- 913 [30] H.C. Matias, F.A. Monteiro Santos, F.E. Rodruiges Ferreira, C. Machado,
914 R. Luzio, Detection of graves using the micro-resistivity method, *Annals of*
915 *Geophys.* 49 (2006) 1235–1244.
- 916
- 917 [31] B.B. Ellwood, D.W. Owsley, S.H. Ellwood, P.A. Mercado-Allinger, P.A.,
918 Search for the grave of the hanged Texas gunfighter, William Preston Longley,
919 *Hist. Arch.* 28 (1994) 94–112.
- 920
- 921 [32] P. Cheetham, Forensic geophysical survey, in, J. Hunter, M. Cox, (Eds.),
922 *Forensic Archaeology: Advances in Theory and Practice*, Routledge, Abingdon,
923 UK, 2005, pp. 62–95.

924

925 [33] J.K. Pringle, J.R. Jervis, Electrical resistivity survey to search for a recent
926 clandestine burial of a homicide victim, UK, *Forensic Sci. Int.* 202 (2010) e1-e7.

927

928 [34] J.K. Pringle, J.R. Jervis, J.D. Hansen, N.J. Cassidy, G.M. Jones, J.P.
929 Cassella, Geophysical monitoring of simulated clandestine graves using
930 electrical and Ground Penetrating Radar methods: 0-3 years, *J. Forensic Sci.*
931 57 (2012b) 1467-1486.

932

933 [35] J.R. Jervis, J.K. Pringle, G.W. Tuckwell, Time-lapse resistivity surveys over
934 simulated clandestine graves, *Forensic Sci. Int.* 192 (2009) 7–13.

935

936 [36] J.L. Kenyon, Ground-penetrating radar and its application to a historical
937 archaeological site, *Hist. Arch.* 11 (1977) 48–55.

938

939 [37] B.W. Bevan, The search for graves, *Geophys.* 56 (1991) 1310–1319.

940

941 [38] J.A. King, B.W. Bevan, R.J. Hurry, The reliability of geophysical surveys at
942 historic period cemeteries: an example from the Plains Cemetery,
943 Mechanicsville, Maryland, *Hist. Arch.* 27 (1993) 4–16.

944

945 [39] M. Watters, J.R. Hunter, Geophysics and burials: field experience and
946 software development, in: K. Pye, D.J. Crofts (Eds.), *Forensic geoscience:*

947 principles, techniques and applications, Geol. Soc. London Spec. Pub. 232
 948 (2004) pp. 21–31.
 949
 950 [40] K. Powell, Detecting human remains using near-surface geophysical
 951 instruments, *Expl. Geophys.* 35 (2004) 88–92.
 952
 953 [41] J.A. Doolittle, N.F. Bellantoni, The search for graves with ground-
 954 penetrating radar in Connecticut, *J. Arch. Sci.* 37 (2010) 941 – 949.
 955
 956 [42] A. Ruffell, Searching for the IRA “disappeared”: ground penetrating radar
 957 investigation of a churchyard burial site, *J. For. Sci.* 50 (2005) 1430-1435.
 958
 959 [43] J.J. Schultz, M.E. Collins, A.B. Falsetti, Sequential monitoring of burials
 960 containing large pig cadavers using ground-penetrating radar, *J. For. Sci.* 51
 961 (2006) 607–616.
 962
 963 [44] J.J. Schultz, Sequential monitoring of burials containing small pig cadavers
 964 using ground-penetrating radar, *J. For. Sci.* 53 (2008) 279–87.
 965
 966 [45] J.K. Pringle, J. Jervis, J.P. Cassella, N.J. Cassidy, Time-lapse geophysical
 967 investigations over a simulated urban clandestine grave, *J. For. Sci.* 53 (2008)
 968 1405-17
 969
 970 [46] J.J. Schultz, M.M. Martin, Controlled GPR grave research: comparison of
 971 reflection profiles between 500 and 250 MHz antennae, *For. Sci. Int.* 209 (2011)
 972 64-69.

973

974 [47] J.L. Davis, J.A. Heginbottom, A.P. Annan, R.S. Daniels, B.P. Berdal, et al.,
975 Ground penetrating radar surveys to locate 1918 Spanish flu victims in
976 permafrost, *J. Forensic Sci.* 45 (2000) 68–76.

977

978 [48] A. Ruffell, B. Kulesa, Application of geophysical techniques in identifying
979 illegally buried toxic waste, *Environ. For.* 10 (2009) 196–207.

980

981 [49] J.K. Pringle, C. Holland, K. Szkornik, M. Harrison, Establishing forensic
982 search methodologies and geophysical surveying for the detection of
983 clandestine graves in coastal beach environments, *For. Sci. Int.* 219 (2012c)
984 e29-e36.

985

986 [50] P. J. Chapman, *Soil and the Environment*, in: J. Holden (Ed.) *An*
987 *Introduction to Physical Geography and the Environment*, Pearson Pubs., 2005.

988

989 [51] D. Fairclough, *Proposed extension: St. James' Church – Unpublished*
990 *intrusive report for Wormseye Ltd.*, 2008.

991

992 [52] R. Cramp, J. Goodwin, A. Davenport, *Archaeological recording and*
993 *exhumation of human remains from St. James' Church, Newchapel,*
994 *Staffordshire. Stoke-on-Trent Arch. Service Report 297*, 2010.

995

996 [53] P. Wessel, W.H.F. Smith, *New, improved version of Generic Mapping Tools*
997 *released*, *Eos Trans. Am. Geophys. Union* 79 (1998) 579.

998

999 [54] G. Stock, The 18th and early 19th century Quaker burial ground at
 1000 Bathford, Bath and north-east Somerset, in M. Cox, (Ed.), Grave Concerns:
 1001 Death and Burial in England 1700-1850. York: Council for British Archaeology
 1002 Research Report 113 (1998) 144-153.
 1003
 1004 [55] J. Litten, The English way of death: the common funeral since 1450, Robert
 1005 Hale Ltd., London, 1992.
 1006
 1007 [56] S. Buteux, R. Cherrington, The excavations in St. Martin's uncovered:
 1008 investigations in the churchyard of St. Martin's-in-the-Bull Ring, Birmingham
 1009 2001, in: M. Brickley, S. Buteux (Eds.), Oxbow Books, Oxford (2006) 24-89.
 1010
 1011 [57] N.J. Tringham, Endon, in: M.W. Greenslade (Ed.), A history of the county of
 1012 Stafford: Leek and the Moorlands, Oxford University Press: Inst. Hist. Res. 7
 1013 (1996) 176-186.
 1014
 1015 [58] R. Speake, The Old Road to Endon, Keele University: Department of Adult
 1016 Education, 1974.
 1017
 1018 [59] Kelly, Directory of the County of Stafford, London: Kelly's Directories Ltd.,
 1019 1921.
 1020

1021 [60] Z. Sutherland, Archaeological recording and exhumation project at St
 1022 Luke's Church, Endon, Staffordshire, Stoke-on-Trent Arch. Service Report 344,
 1023 2012.
 1024

1025 [61] G. Taylor, A parish in perspective: a history of the church and parish of St.
 1026 John of Jerusalem South Hackney, London, 2002.
 1027

1028 [62] G.M. Jones, N.J. Cassidy, P.A. Thomas, S. Plante, J.K. Pringle, Imaging
 1029 and monitoring tree-induced subsidence using electrical resistivity tomography,
 1030 Near Surf. Geophys. 7 (2009) 191-206.
 1031

1032 [63] J.S. Mellet, Location of human remains with ground penetrating radar, in P.
 1033 Hanninen, S. Autio, (Eds.), Proc. 4th Int. Conf. GPR, June 8-13; Rovaniemi,
 1034 Geol. Surv. Finland Spec. Paper 16 (1992) 359–365.
 1035

1036 [64] A. Ruffell, J. McKinley, Geoforensics, Wiley Pubs, UK, 2008, 332pp.
 1037

1038 [65] M. Cox, J.R. Hunter, Forensic archaeology, Taylor & Francis Pubs, UK,
 1039 2005.
 1040

1041 [66] C. Vaughan, Ground penetrating radar surveys used in archaeological
 1042 investigations, Geophys. 51 (1986) 595–604.
 1043

1044 [67] L.B. Conyers, Ground penetrating radar techniques to discover and map
 1045 historic graves, Hist. Arch. 40 (2006) 64–73.

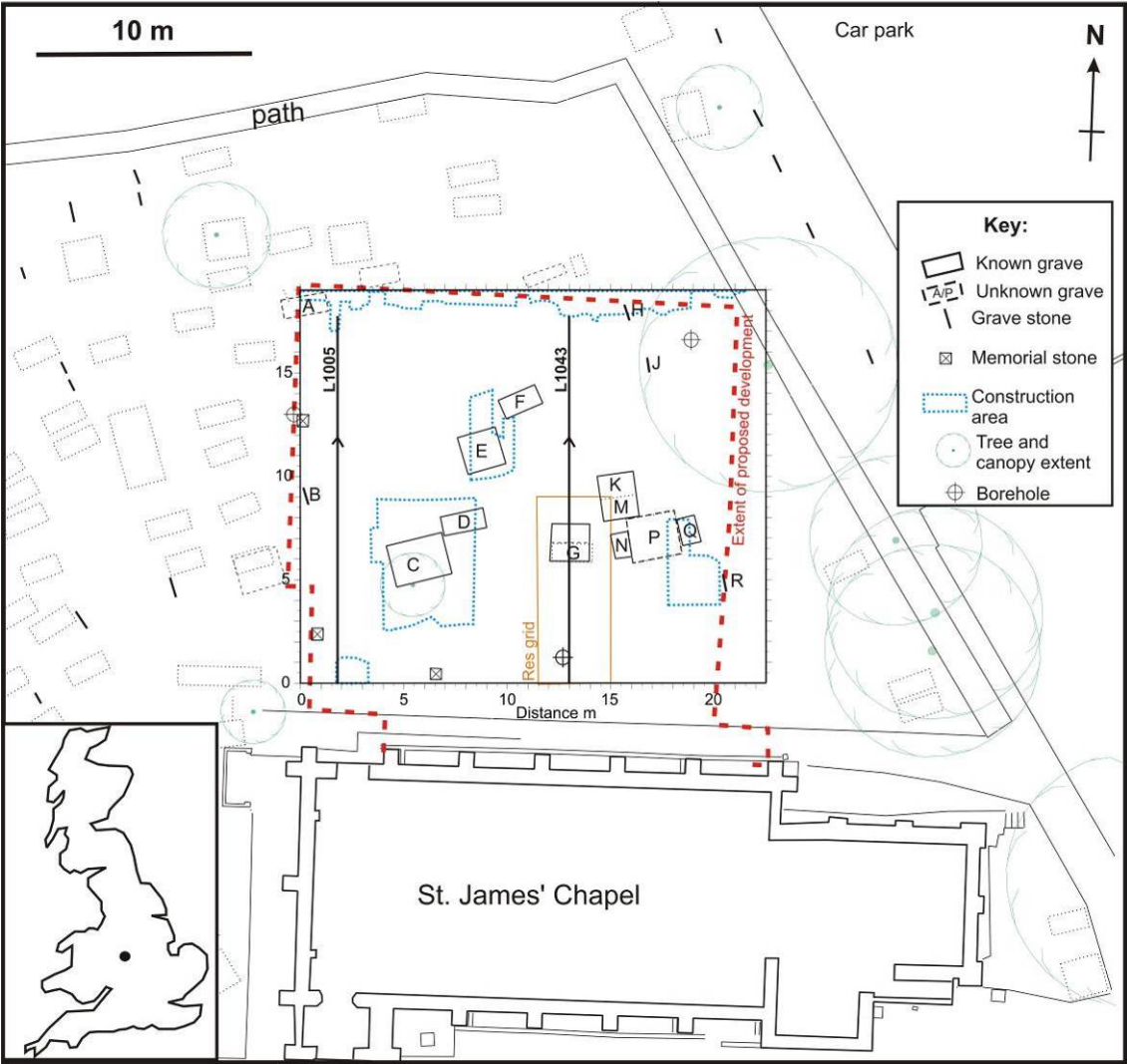
1046

1047 [68] M. Harrison, L.J. Donnelly, Locating concealed homicide victims:
1048 developing the role of geoforensics, in: K. Ritz, L. Dawson, D. Miller (Eds.),
1049 Criminal and Environmental Soil Forensics, Springer, Dordrecht, 2009, pp. 197–
1050 219.

1051

1052

1053 **10. Figures**



1054
1055 **Fig. 1.** Mapview of case study 1 with location map (inset). Proposed building
1056 foot-print, geophysical survey grid, trial GPR profile and grave positions shown
1057 (see key).



Fig. 2. Photographs of case study 1 site, also showing (A) 225 MHz dominant frequency GPR and (B) bulk ground resistivity (0.5 m fixed-offset) data being collected. Note trial 2D GPR L1043 profile position over burial vault (Fig. 3b) marked in (B).

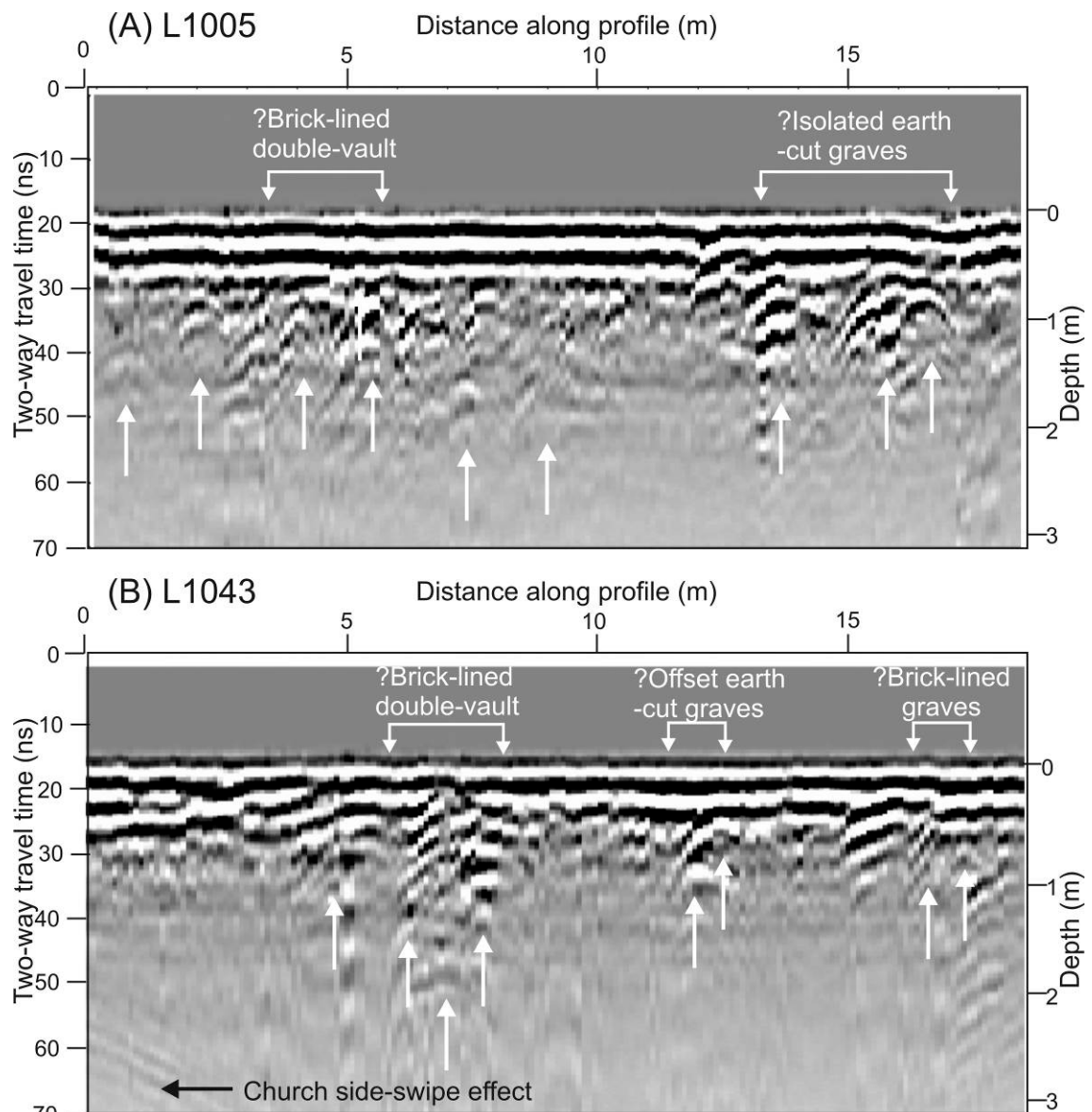


Fig. 3. Processed 225 MHz 2D GPR profiles (A) L1005 and (B) L1043 (Fig. 1 for location) with target positions (arrows) and their interpretations annotated. Note the top 1 m of top soil was removed before geophysical surveying (see text).

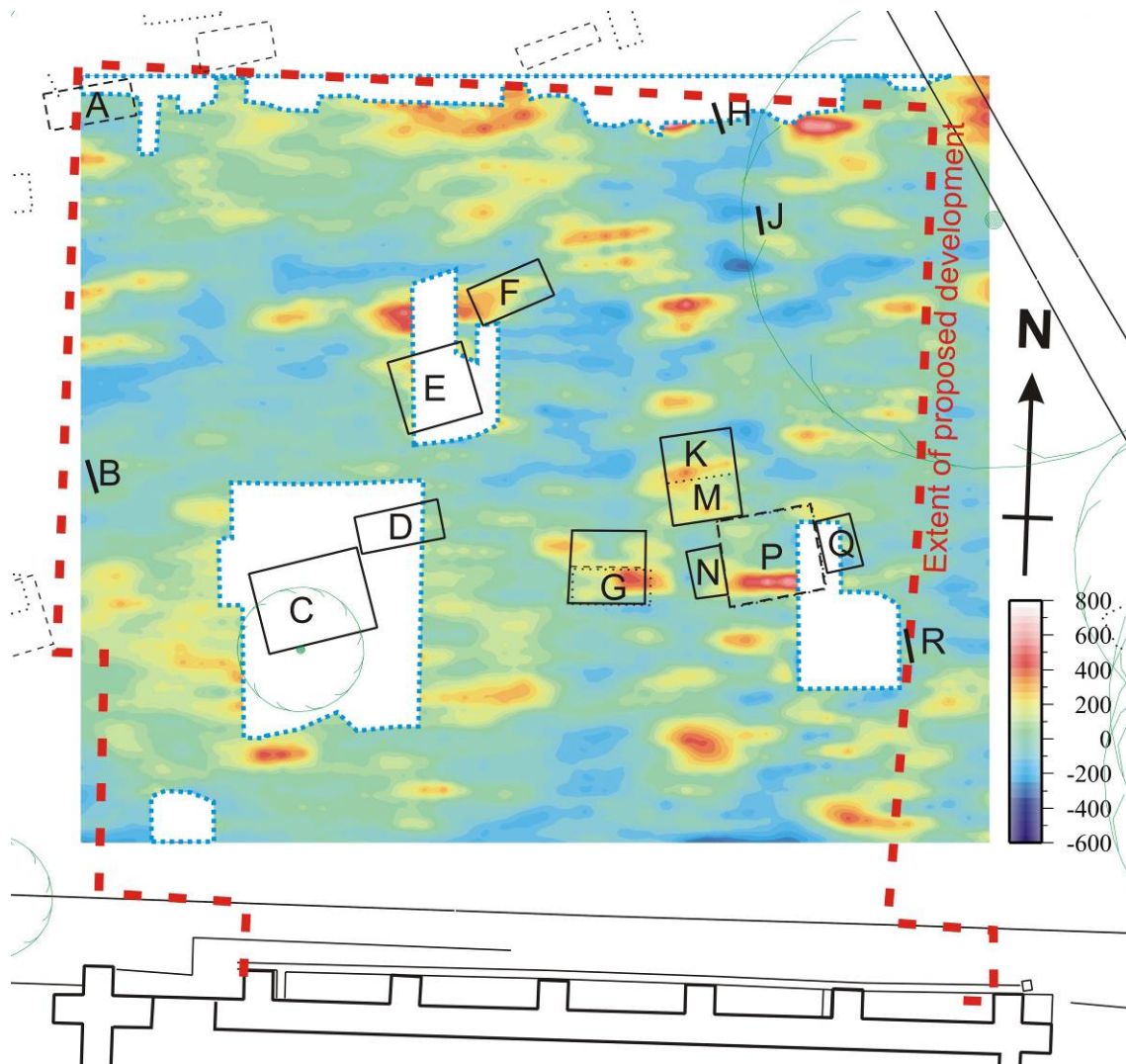


Fig. 4. Mapview of 225 MHz GPR absolute amplitude 0-80 ns time-depth slice with background map. White areas indicate where 2D profiles could not be acquired.

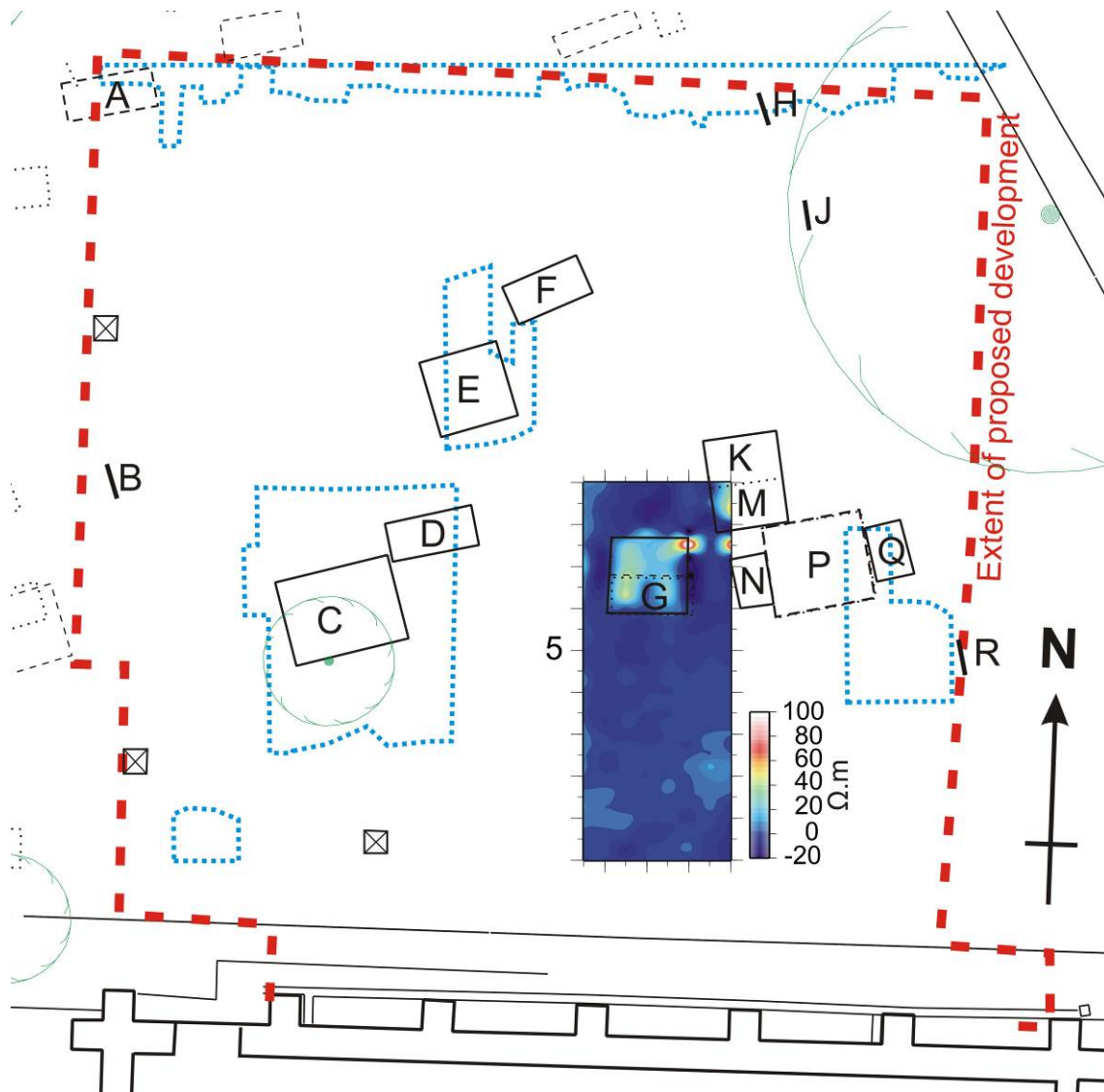


Fig. 5. Map view of processed bulk ground resistivity data with background map.

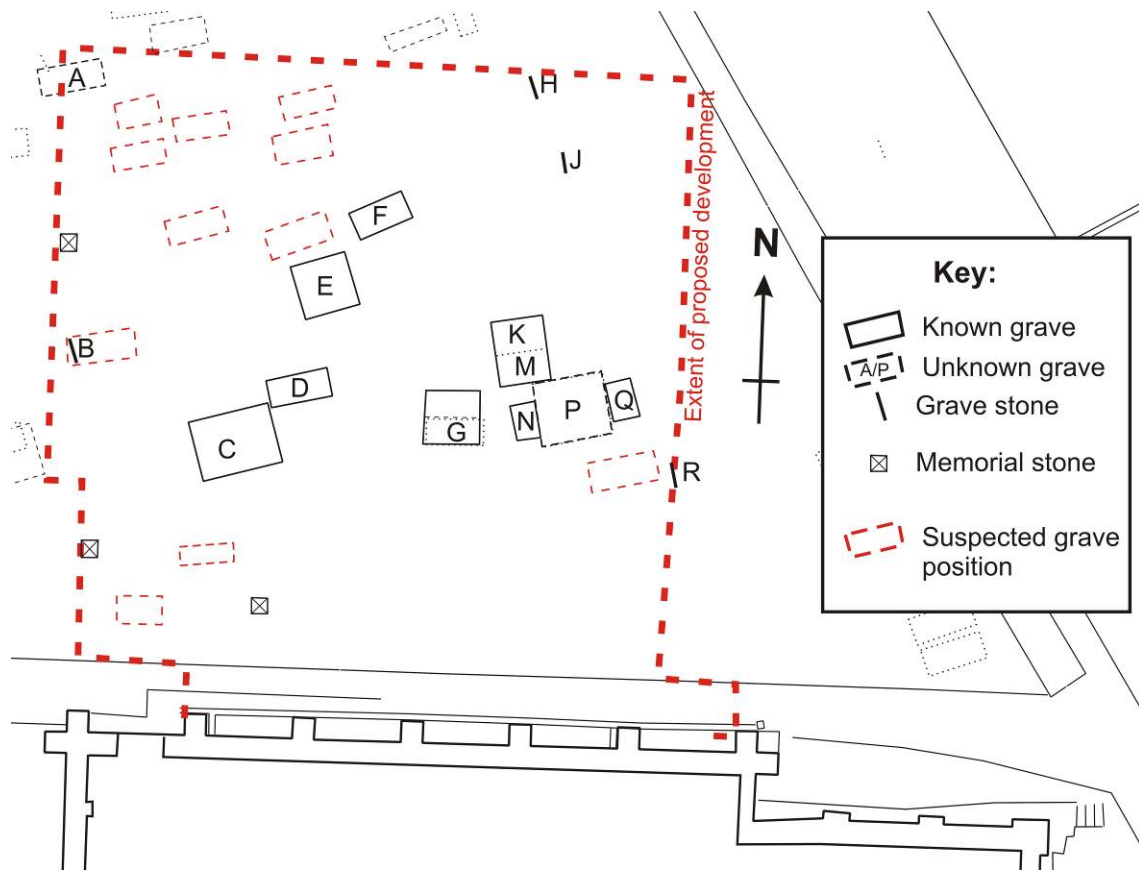


Fig. 6. Case study 1 summary of known and unknown grave/vault positions.



1077

1078 **Fig. 7.** Case Study 1 archaeology excavation photographs of (A) single brick-
 1079 lined grave H and (B) double brick lined family vault C with 0.5 m scale bars.

1080 See Table 2 for details.

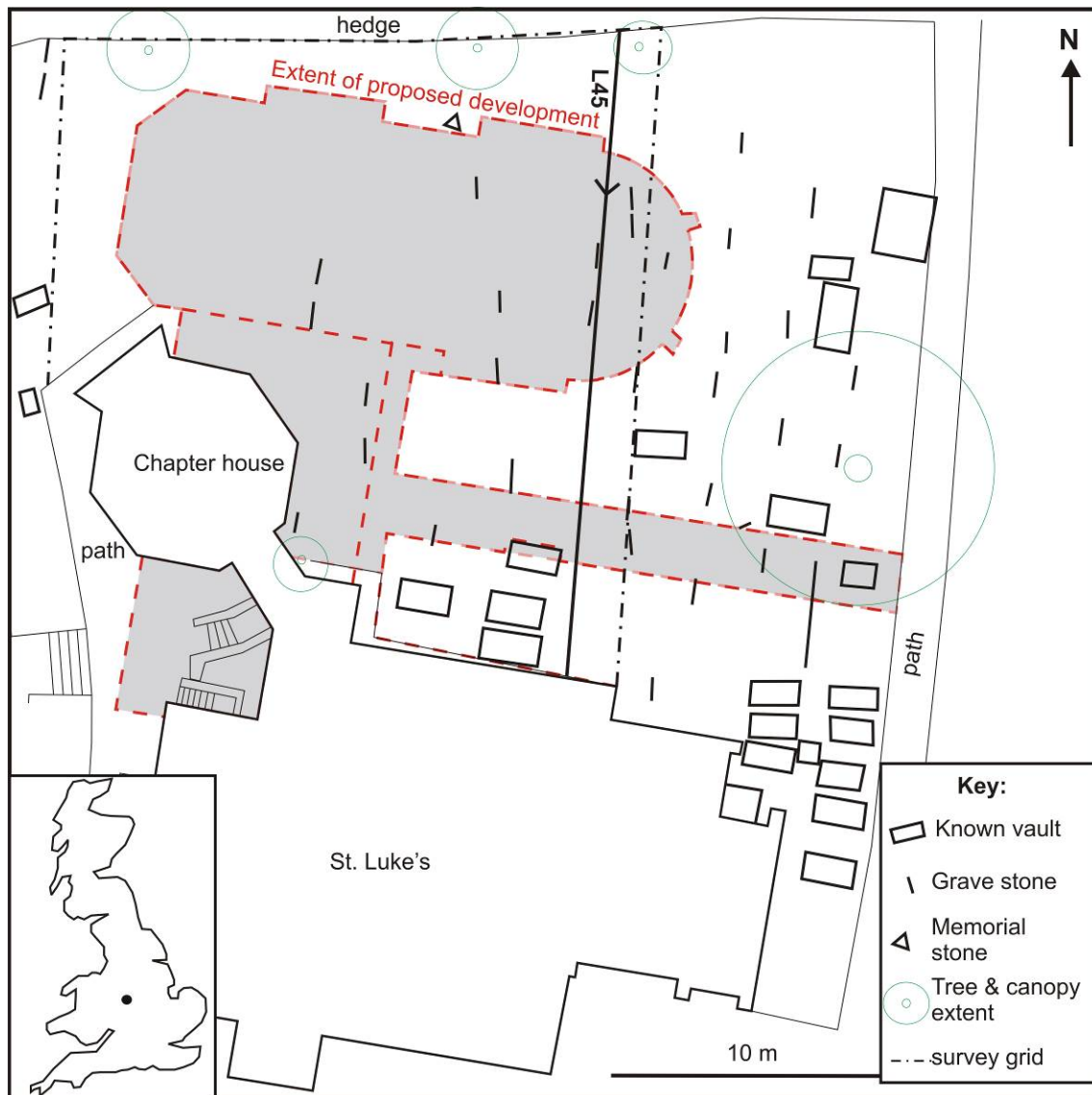


Fig. 8. Map view of St. Luke's Church, Endon, Staffordshire study site with location map (inset). Proposed building footprint (red rectangle) position shown (see key).

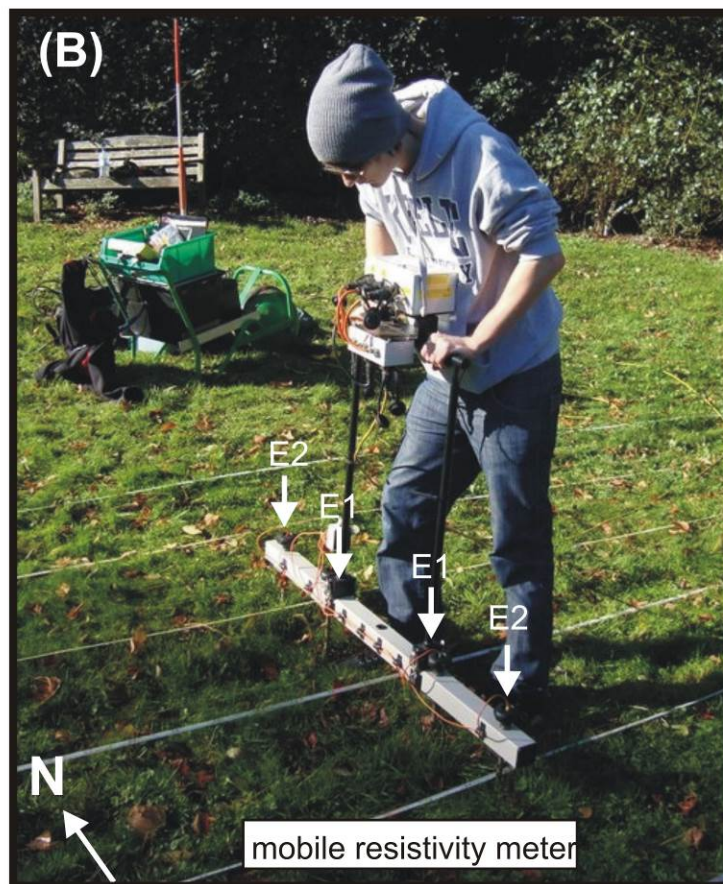
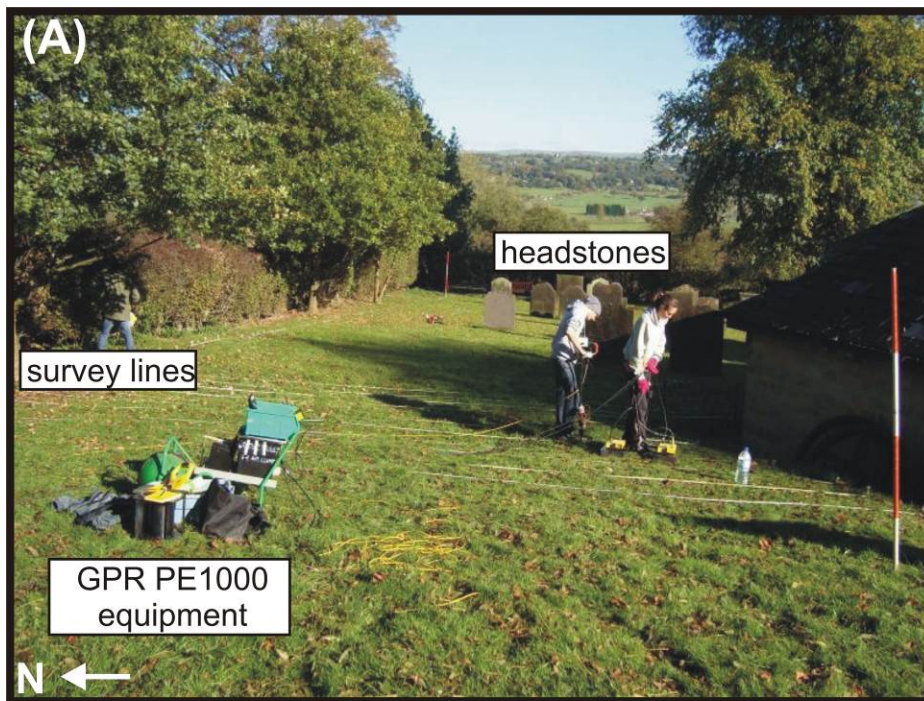


Fig. 9. Photographs of case study 2 site, also (A) 225 MHz dominant frequency GPR and (B) bulk ground resistivity 0.5 m (E1) and 1 m (E2) fixed-offset data being collected.

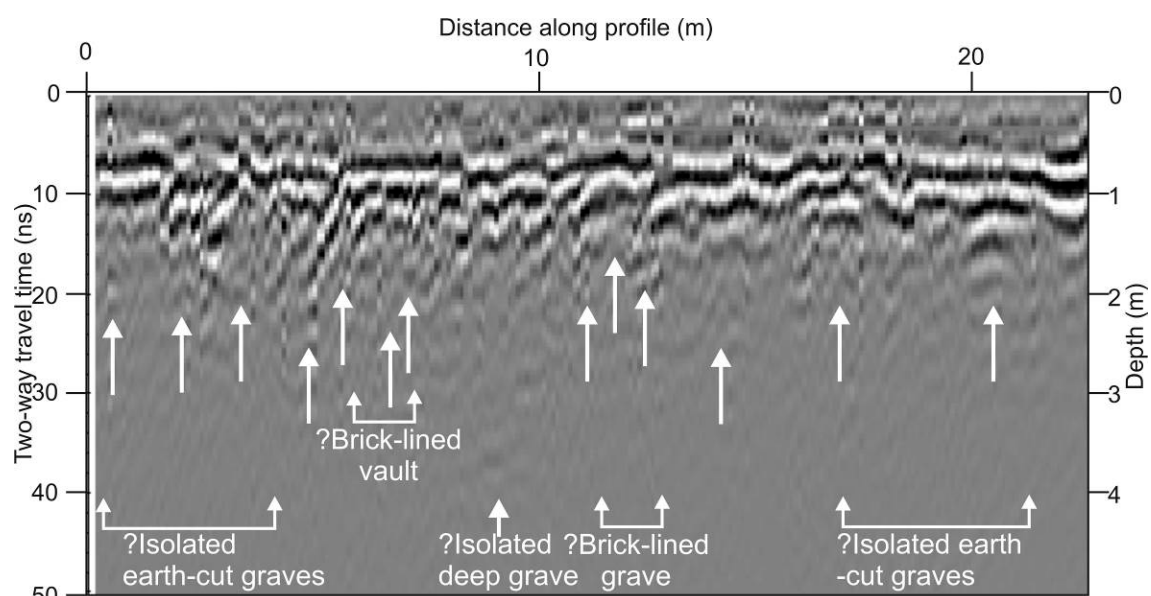


Fig. 10. (A) Processed 225 MHz 2D GPR profile L45 (Fig. 8 for location) with target positions (arrows) and their interpretations annotated.

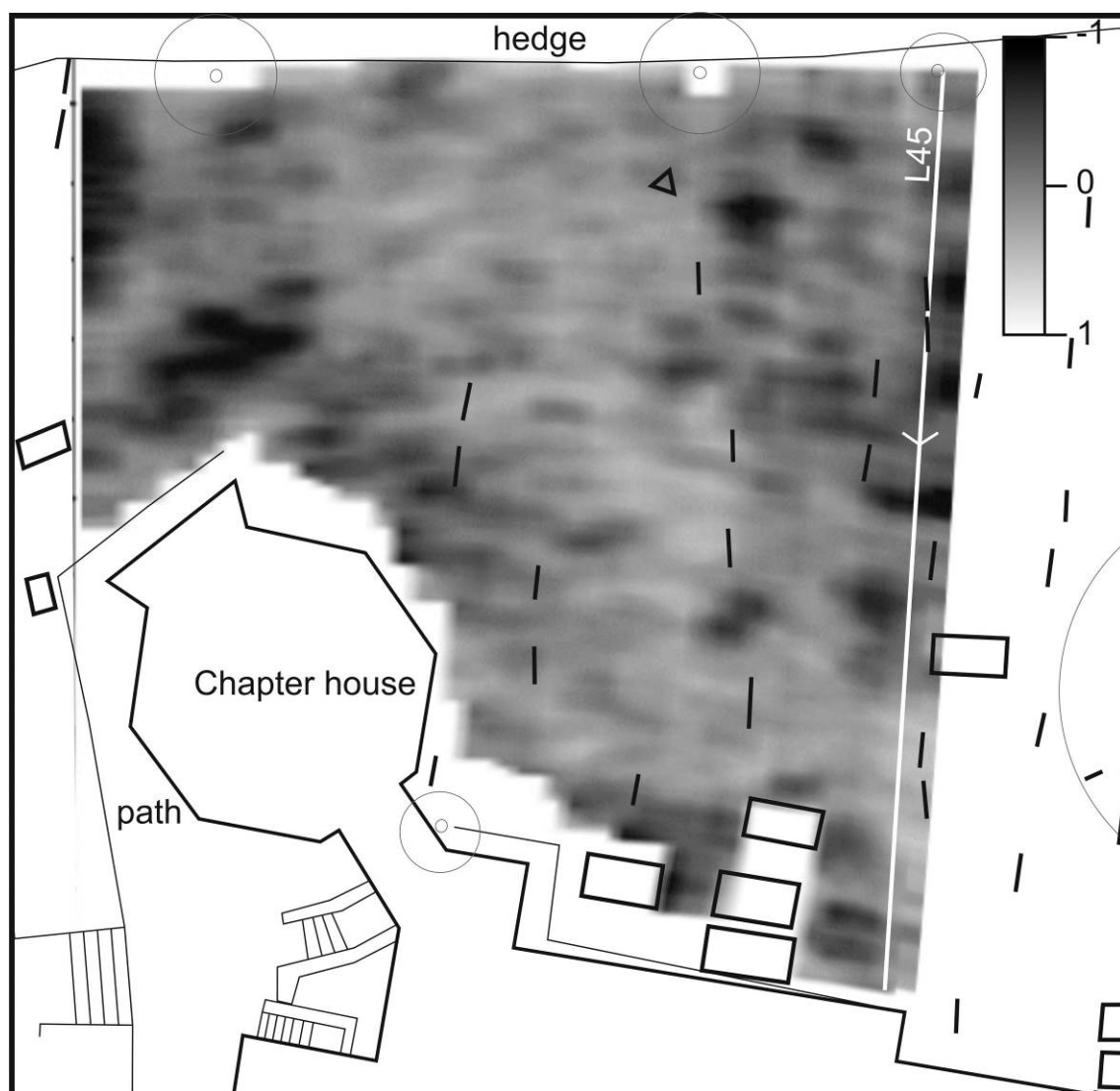


Fig. 11. Mapview of 225 MHz GPR absolute amplitude 20-40 ns time-depth slice with background map.

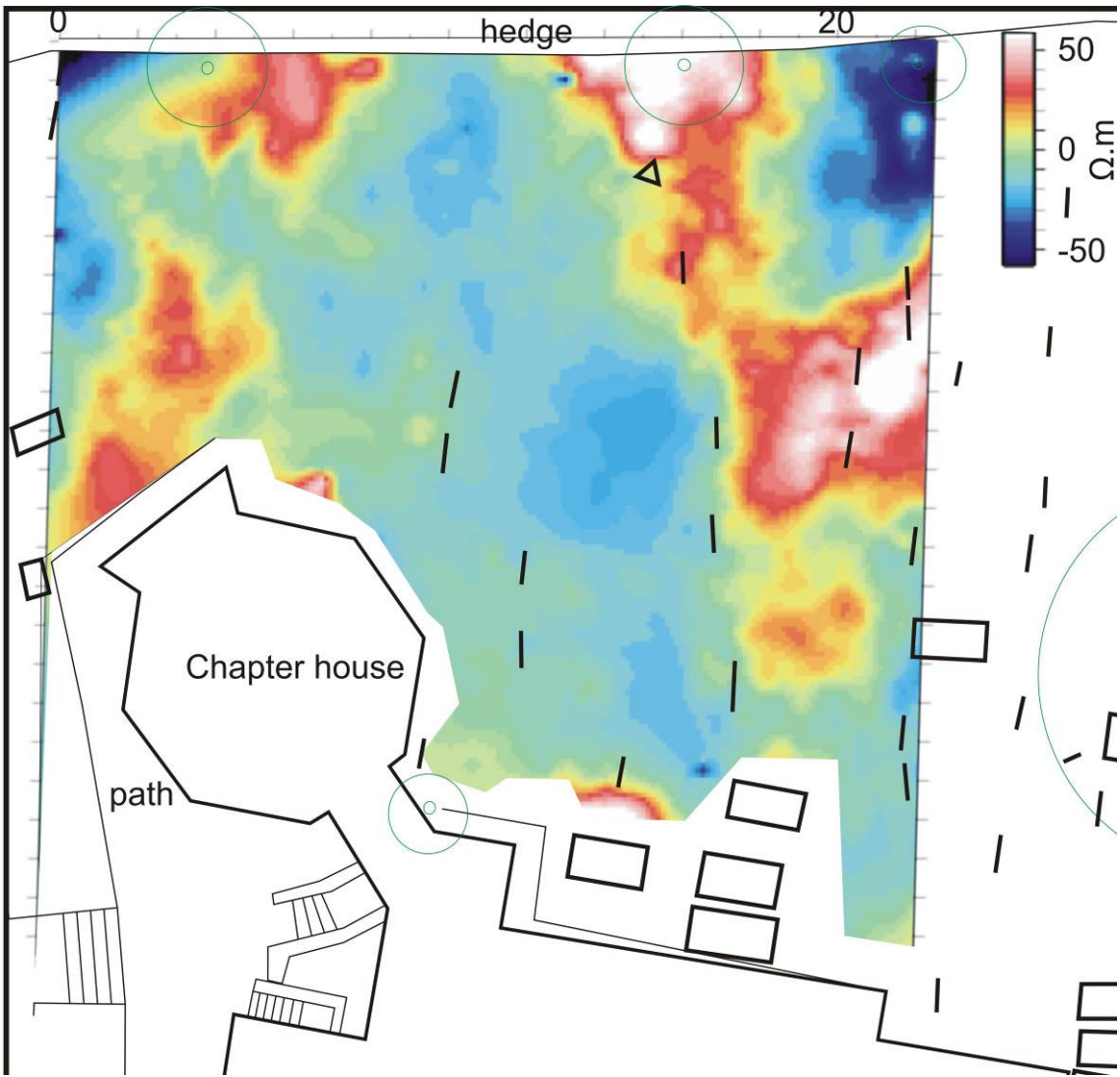


Fig. 12. Map view of the processed bulk ground resistivity (0.5 m fixed-offset) probe spacing dataset with background map.



1098

1099 **Fig. 13.** Case study 2 summary of known and unknown grave/vault positions.

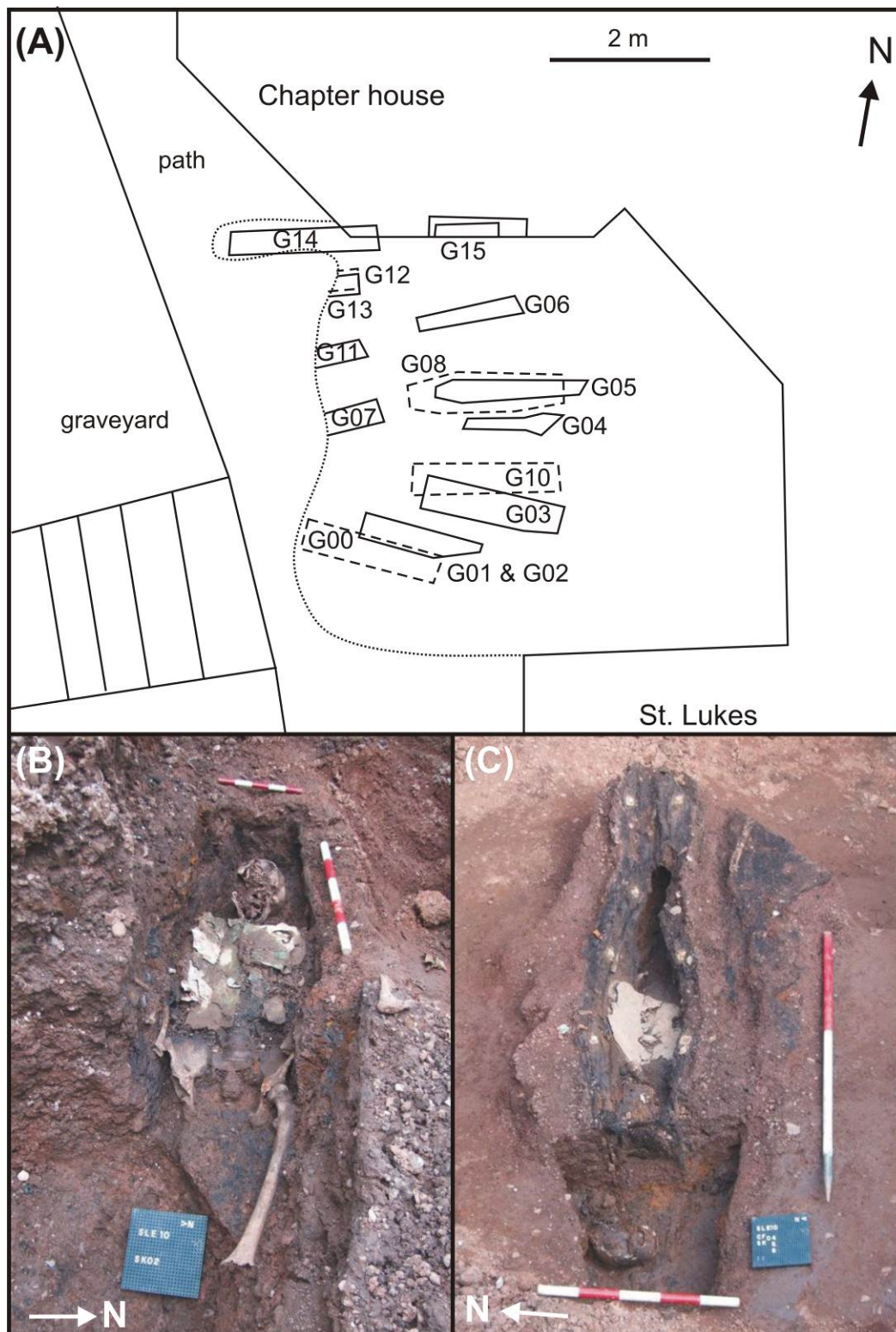


Fig. 14. Case Study 2 archaeological excavation; (A) map, (B) G02 and; (C) G5/08 photographs of earth-cut graves with 0.5 m scale bars. See Table 3 for details.

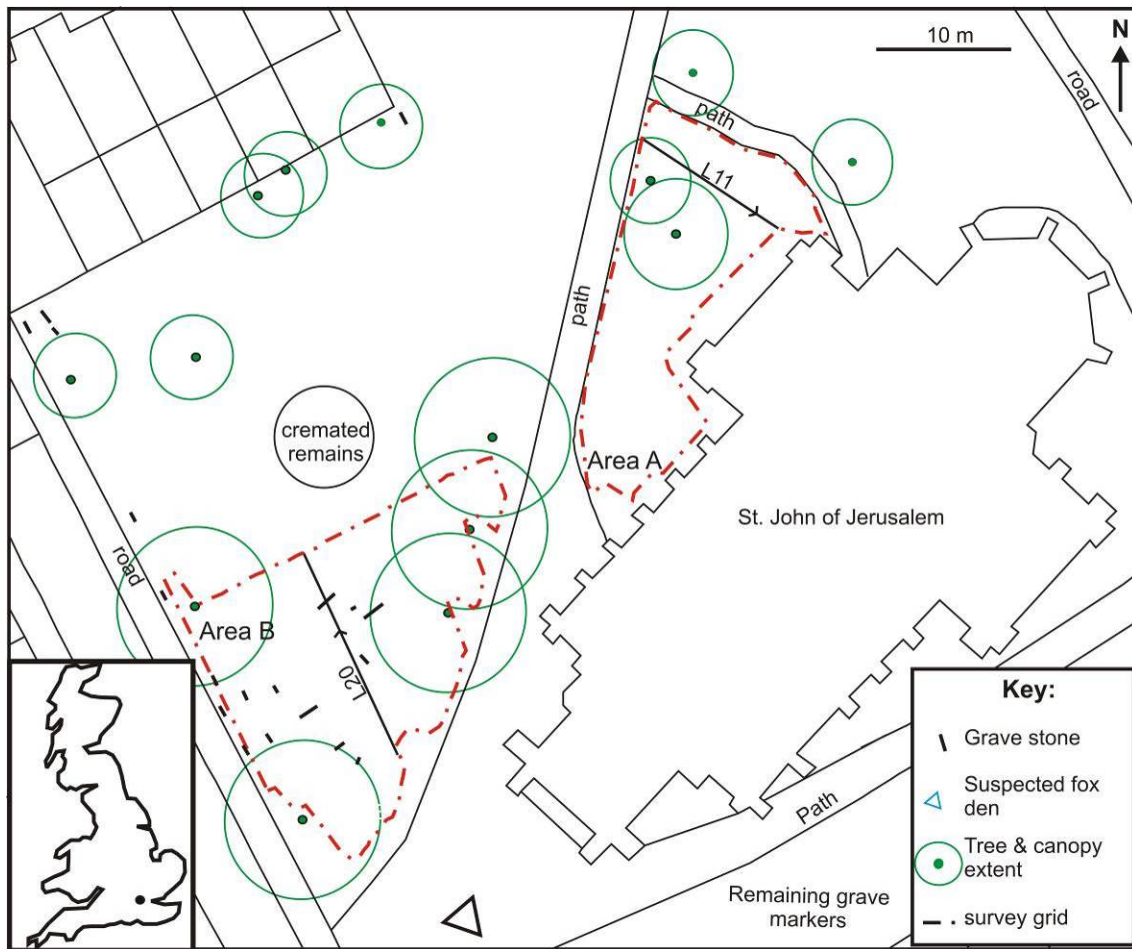


Fig. 15. Mapview of case study 3 with location map (inset). geophysical survey areas A and B and grave positions shown (see key).

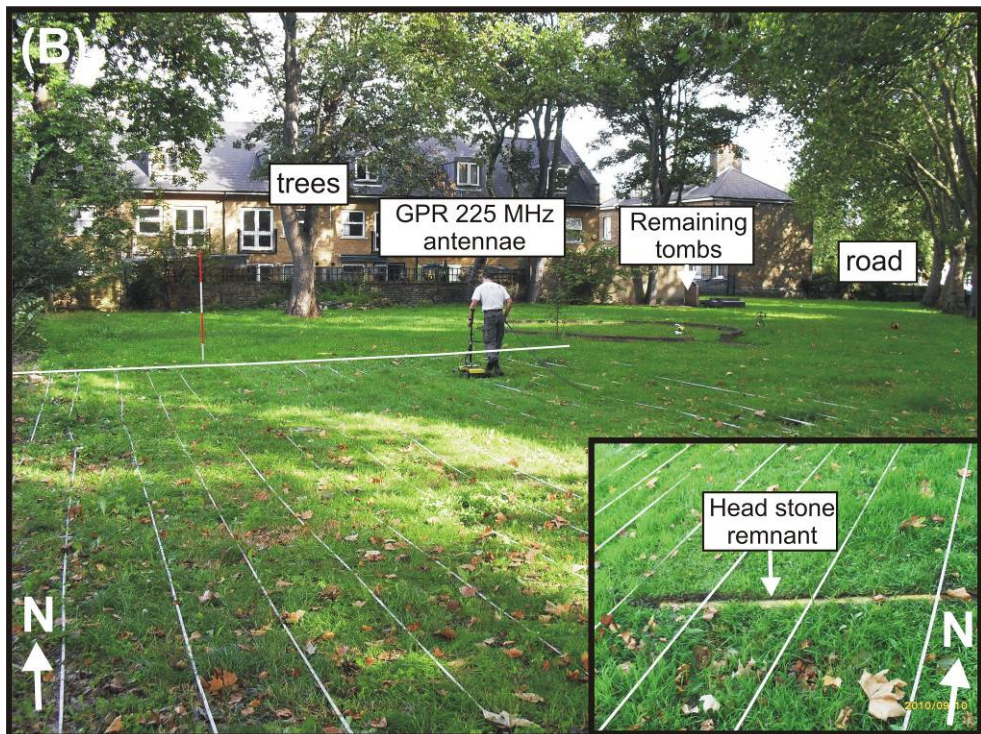
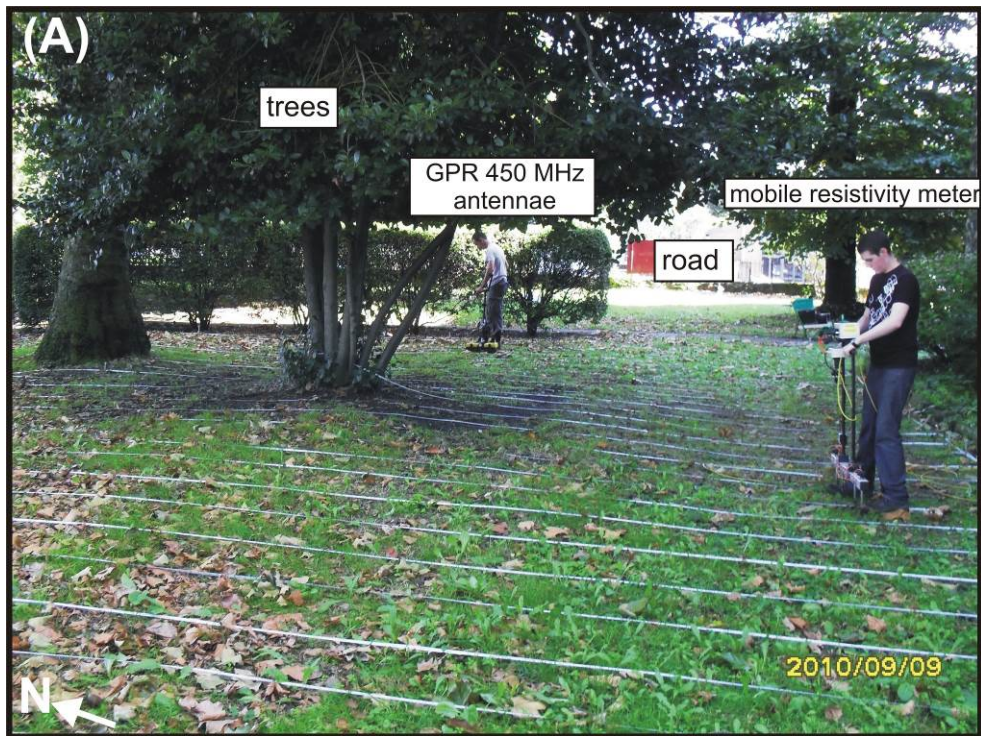


Fig. 16. Photographs of case study 3 site of (A) Area 1 and (B) Area 2 with remnant headstone (inset). GPR and bulk ground resistivity (0.5/1 m) fixed-offset data collection also shown.

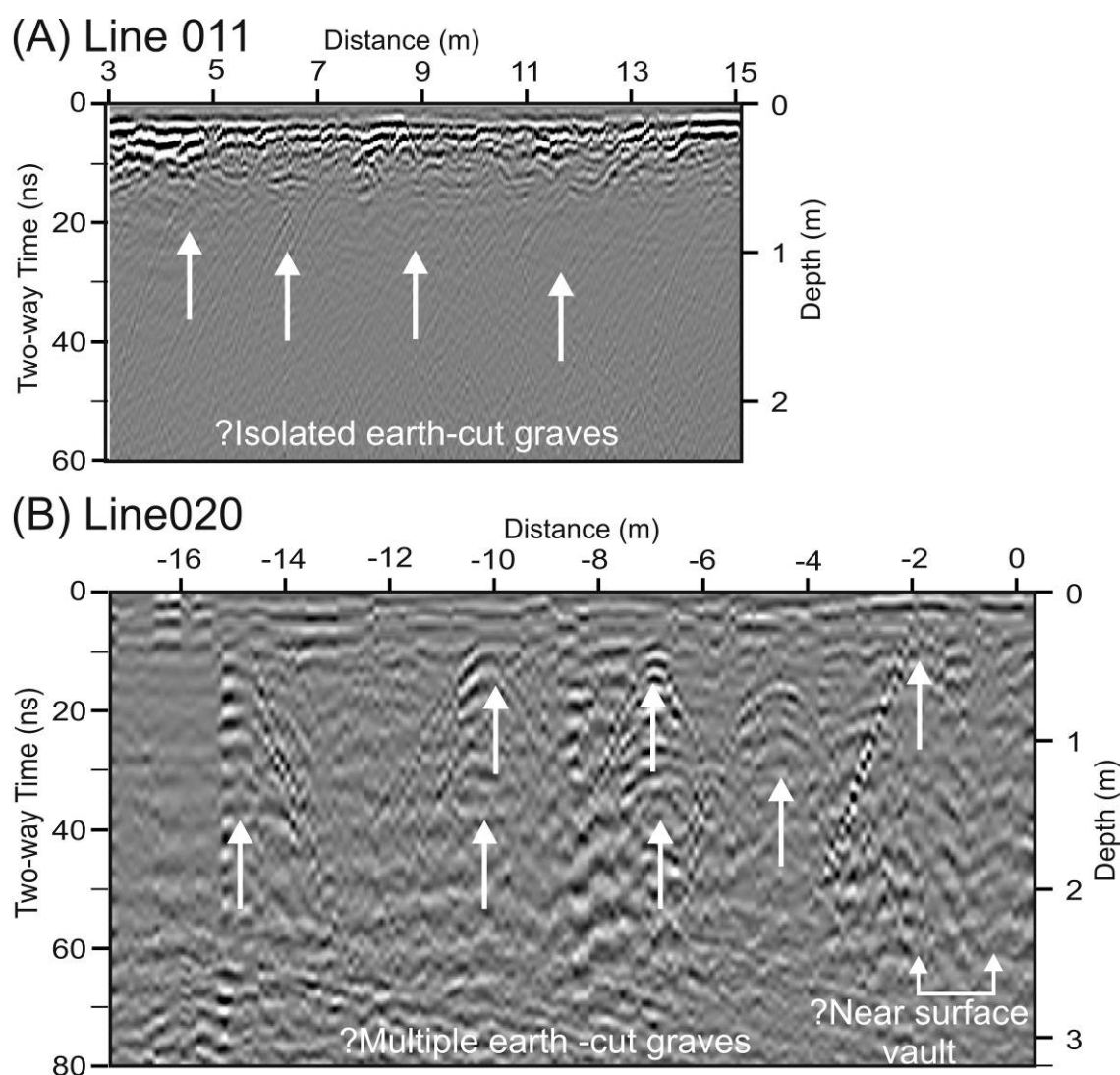


Fig. 17. (A) Processed 450 MHz 2D GPR profile L11 from Area A and 225 MHz 2D GPR profile L23 from Area B (Fig. 15 for location) with target positions (arrows) and their interpretations annotated.



Fig. 18. Mapview of combined 225/450 MHz GPR absolute amplitude 9-35 ns time-depth slices with background map.

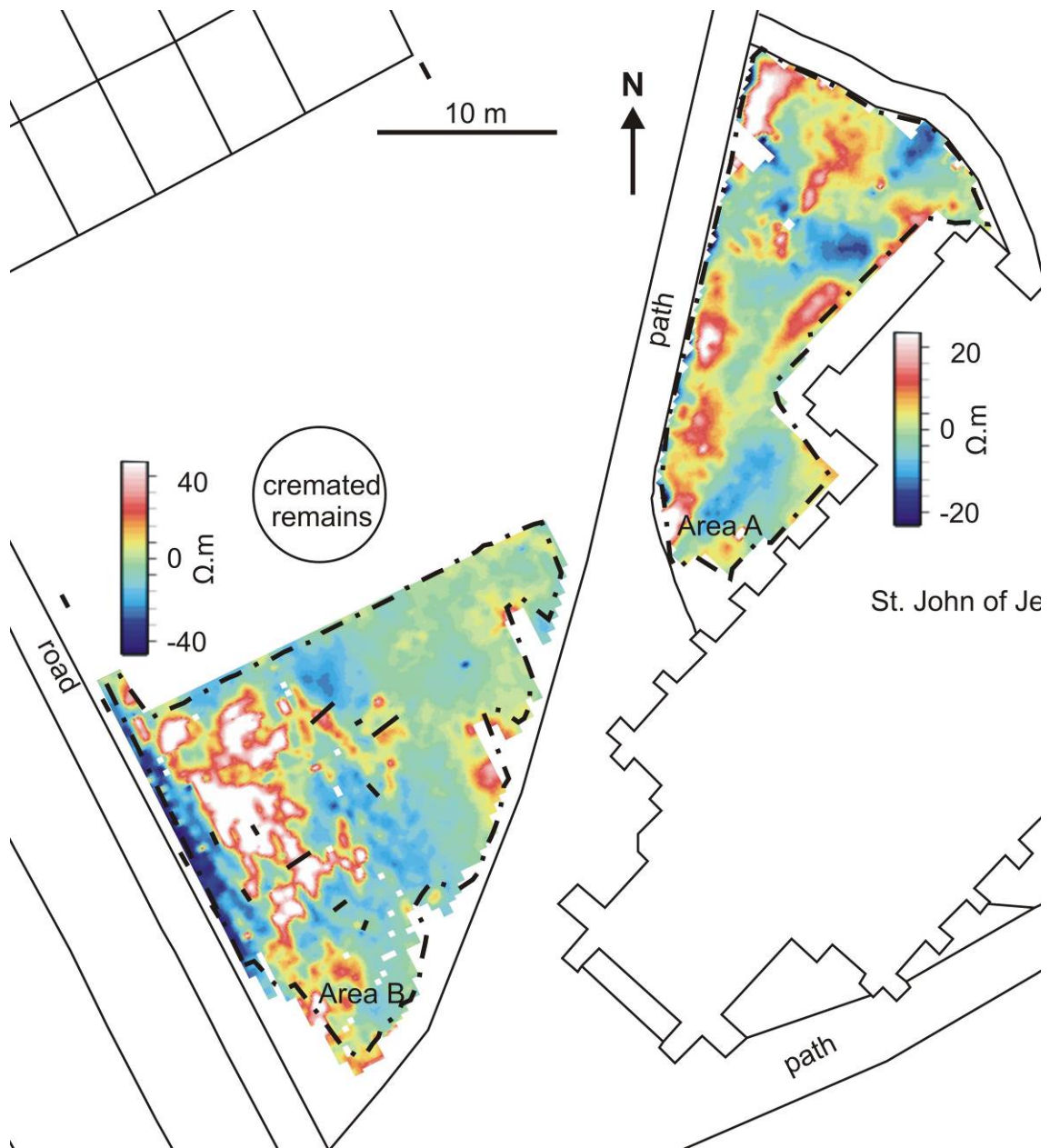


Fig. 19. Map view of the processed bulk ground resistivity (0.5 m fixed-offset) probe spacing dataset with background map. See respective area keys.

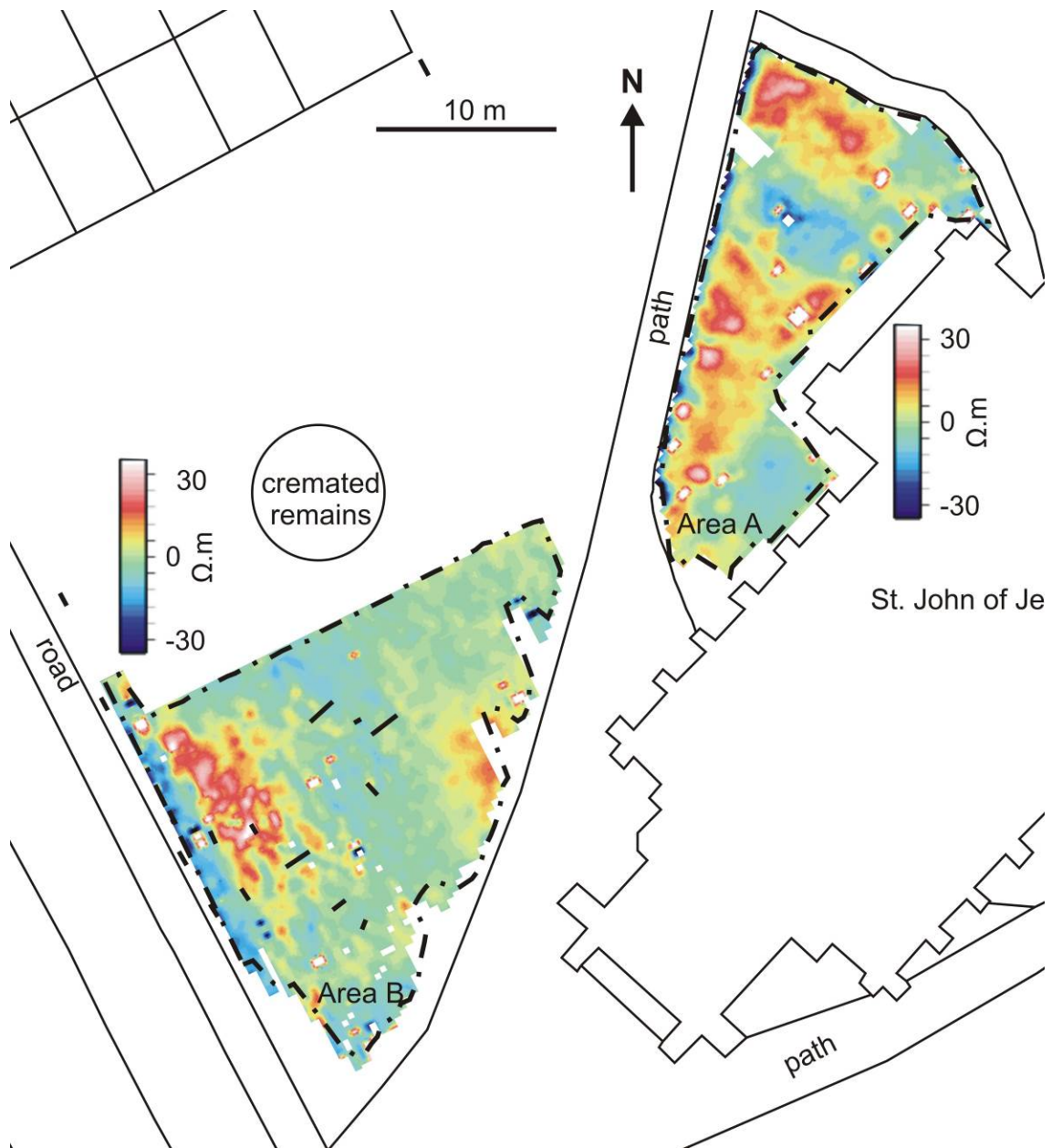


Fig. 20. Map view of the processed bulk ground resistivity (1 m fixed-offset) probe spacing dataset with background map. See respective area keys.

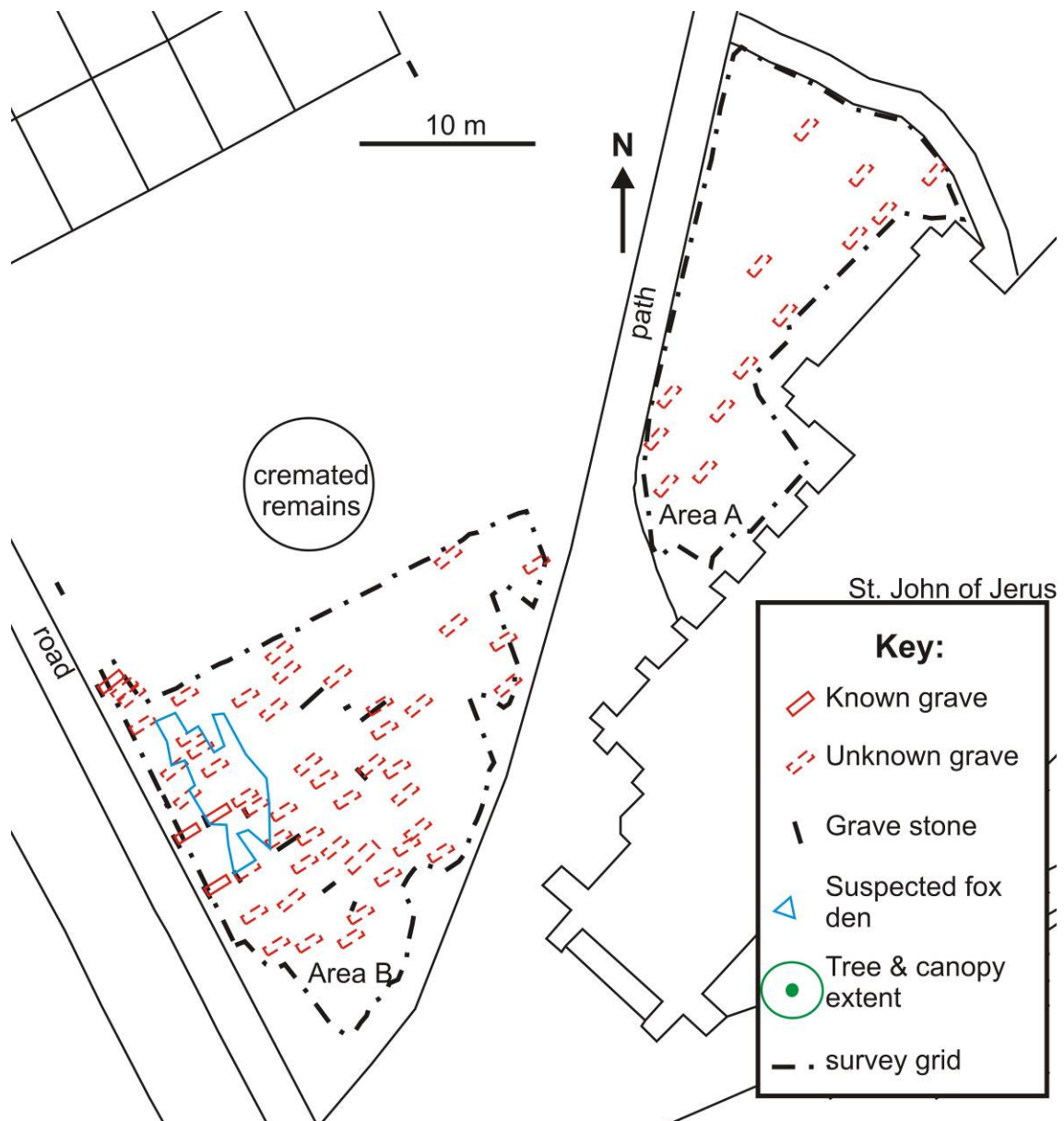


Fig. 21. Case study 3 summary of known and unknown grave/vault positions.

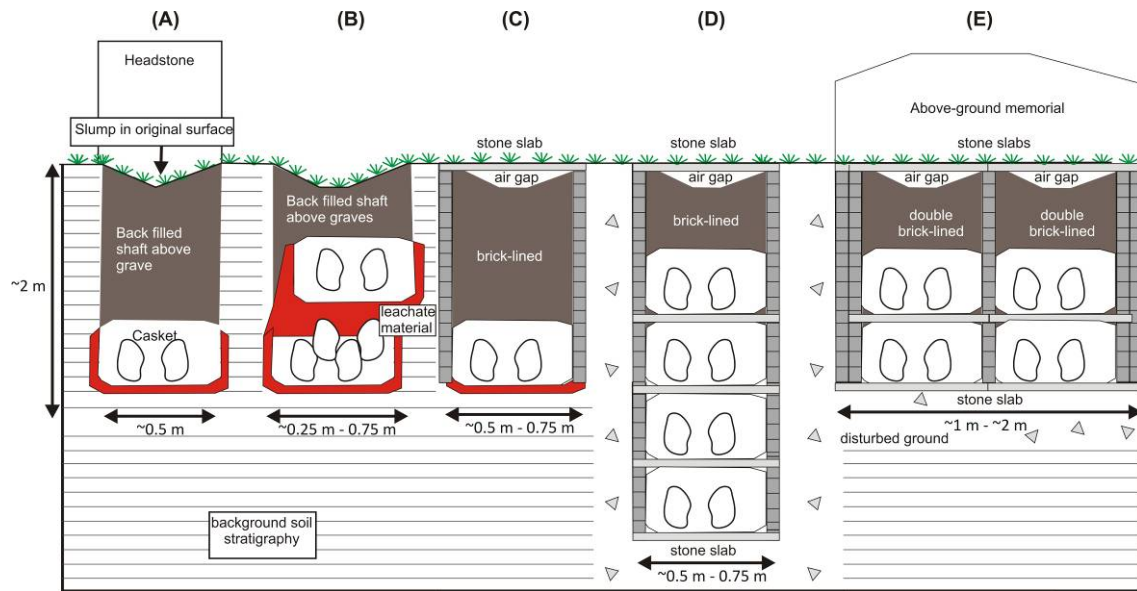


Fig. 22. Generalised schematic of burial styles encountered in the three case studies discussed showing (left to right): (A) isolated earth-cut grave (e.g. see Fig. 10); (B) multiple earth-cut graves (e.g. see Fig. 17b); (C) isolated brick-lined & top slab grave (e.g. see Fig. 10); (D) multiple brick-lined & top slabbed graves (e.g. see Fig. 3a) and; (e) multiple brick-lined and top slabbed grave vault (e.g. see Fig. 3b).

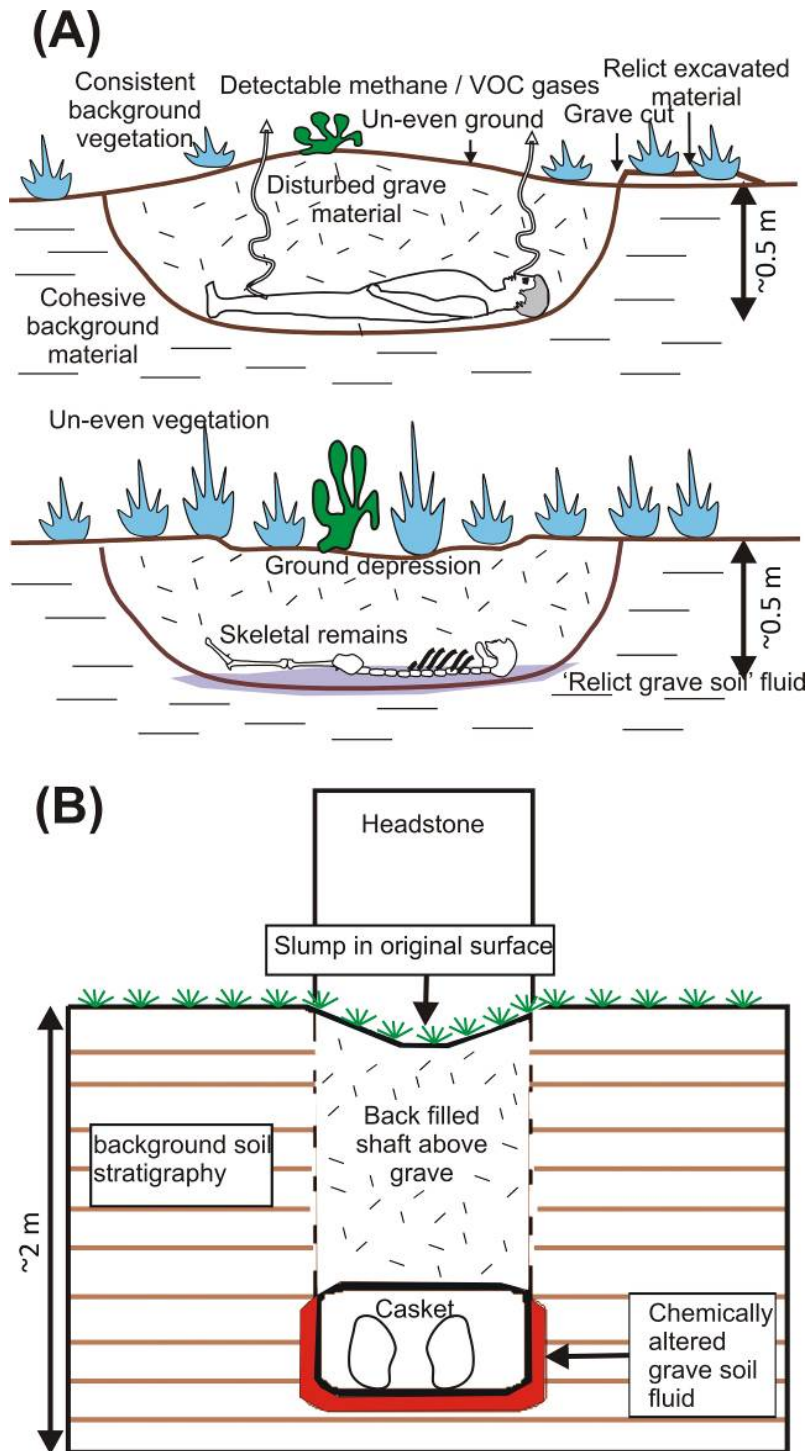


Fig. 23. Generalised schematics of (A) typical clandestine grave of an isolated murder victim with temporal changes (modified from [17 Pringle et al. 2012a]) and (B) an isolated earth-cut grave burial in a cemetery or graveyard, with (1) post-burial soil, (2) shaft, (3) coffin and (4) contents identified geophysical targets named by [67 Conyers 1986].

1144 **11. Tables**

Grave	No. of individuals	Burial Dates
A	Unknown	Unknown – not marked
B	6	1822, 1832, 1834, 1845, 1847, 1874.
C	8	1821, 1831, 1851, 1877, 1880, 1885, 1895, 1913.
D	4	1919, 1943, 1962, 1966.
E	13	1824, 1830, 1832, 1842, 1849, 1860, 1864, 1871, 1873, 1875, 1887, 1900, 1908.
F	2	1827, 1833.
G	5	1842, 1846, 1853, 1867, 1876.
H	3	1834, 1834, 1887.
J	1	1874
K	3	1881, 1882, 1895.
L	3	1846, 1868, 1874.
N	8	1817, 1824, 1854, 1867, 186(-9?), 1870, 1878, 1879.
P	Unknown	Unknown – not marked
R	4	1869, 1876, 1916.

1145

1146 **Table 1.** Summary of case study 1 expected burials (locations shown in Fig. 2).

Grave / Vault & No.	Dimen-sions*	Contents & burial date	Detailed description
---------------------	--------------	------------------------	----------------------

Earth-cut grave A	2.2 m x 0.75 m x 0.85 m	1 adult, unknown	Wood coffin rotted but skeletal remains in good condition
Vault C	2.10 m x 1.35 m x 0.9 m deep	3 adults & 1 juvenile, 1880 - 1913	Crudely lime-mortar jointed, double- skinned red brick walls. Slate roof with 3 stone capping slabs ~0.15 m thick. Wood coffins completely rotted, skeletal remains varied from 2 complete & 2 poor.
Brick-lined grave Ea	2.5 m x 0.25 m x 1.25 m deep	2 adults, 1873 & 1887.	Curvilinear in shape (following coffin), 1 red brick thick wall, horizontal flagstone in between. Wood coffins rotted but skeletal remains in fair condition.
Brick-lined grave Eb	2.5 m x 0.25 m x 1.25 m deep	1 adult, 1908	Curvilinear, one red brick thick lined. Wood coffin rotted but skeletal remains in good condition
Brick-lined grave H	2.6 m x 0.25 m x 0.75 m deep	1 adult, 1887	Curvilinear, one red brick thick lined, with sandstone slab atop. Wood coffin rotted but skeletal remains in fair condition.

Table 2. Relevant archaeological characteristics of the case study 1 excavated burials. Condition categories for human remains: Good = bones complete, Fair = bones mostly complete, Poor = Bones incomplete and/or damage/erosion. Burial letter locations marked in Fig. 4. *Note depths were on excavation after removal of 1.4 m topsoil.

Grave No.	Dimensions	Contents & burial date	Coffin & individual description
G01/2 Fig. 15	2.0 m x 0.5 m x 0.8 m bgl	2 adults (unknown)	Wood coffins completely rotted, skeletal remains fair & disturbed
G03	2.0 m x 0.25 m x 0.8 m bgl	1 adult d. 1963	Wood coffin, skeletal remains fair
G04	1.5 m x 0.25 m x 0.8 m bgl	1 adult, d. 1894?	Wood coffin stain only, incomplete set skeletal remains poor.
G05/8 Fig. 15	2.00 m x 0.5 m x 0.9 & 1.2 m bgl	2 adults	Wood coffin rotten, adipocere present, skeletal remains fair
G06	1.5 m x 0.25 m x 1.2 m bgl	1 adult	Wood coffin fragments, incomplete skeletal remains poor & disturbed
G07	0.6 m x 0.3 m x 0.8 m bgl	1 adult, d. 1875?	Coffin stain only, no surviving human remains
G09	2.0 m x 0.5 m x 1.0 m bgl	1 adult, below G02	Wood coffin rotten, skeletal remains poor
G10	2.0 m x 0.5 m x 1.15 m bgl	1 adult, below G03	Coffin stain only, skeletal remains poor & disturbed
G11	0.5 m x 0.25 m x 0.8 m bgl	1 adult, d. 1926?	Coffin stain only, no surviving human remains
G12/13	0.5 m x 0.25 m x 1.0 m bgl	2 juveniles	Wood coffin fragments, incomplete skeletal remains poor
G14	2.0 m x 0.75 m x 1.25 m bgl	1 adult	Wood coffin fragments, incomplete skeletal remains poor & disturbed
G15	1.0 m x 0.25 m x 1.1 m bgl	1 adult	Wood coffin fragments, incomplete skeletal remains good

Table 3. Relevant archaeological characteristics of the case study 2 excavated burials. Individual conditions: Good = bones complete, Fair = bones mostly complete, Poor = bones incomplete and/or damage/erosion.

Burial style	GPR characteristic (2D profile)	Electrical resistivity characteristic (mapview)
(A) Isolated earth-cut graves	Clear $\frac{1}{2}$ hyperbolic reflection (Fig. 20b)	Isolated rectangular relative high/low anomaly (Fig. 20)
(B) Multiple occupancy earth-cut graves	Multiple clear $\frac{1}{2}$ hyperbolic reflections stacked vertically (Fig. 17b)	Isolated rectangular relative high/low anomaly (Fig. 20)
(C) Isolated brick-lined grave	Near-surface narrow reflection events either side of a clear $\frac{1}{2}$ hyperbolic reflection event (Fig. 10b)	Isolated rectangular relative high anomaly (Fig. 20)
(D) Multiple brick-lined & top slab graves	Near-surface narrow reflection events either side of multiple clear $\frac{1}{2}$ hyperbolic reflection events (Fig. 10)	Large isolated rectangular relative high anomaly (Fig. 20)
(E) Multiple brick-lined & top slab vault	Near-surface narrow reflection events either side of multiple clear $\frac{1}{2}$ hyperbolic reflection events (Fig. 10)	Large isolated large rectangular relative high anomaly (Fig. 5)

1155 **Table 4.** Generalised burial styles encountered in this study (see Fig. 22) and
1156 their geophysical responses. Note burial age and soil type has not been
1157 factored into this table.

1158